Towards Low Emissions Operation of 65 and 200kW Recuperated Gas Turbine Engines on 100% Hydrogen

SCG Agreement 5660068119

Prepared by: **W. Villatoro, O. Aguilar-Cerna, J. Slope, and V.G. McDonell**

Submitted by:

Professor Vincent McDonell, Director
UCI Combustion Laboratory
University of California, Irvine
131 Engineering Laboratory Facility
Irvine, California 92697-3550
Tel: (949) 824-5950 x121
Fax: (949) 824-7423
mcdonell@ucicl.uci.edu

Draft: 30 November 2023
Revision: 5 Feb 2024
Rev2: 6 Feb 2024
Rev3: 7 Feb 2024

Contents

EXECUTIVE SUMMARY **1**

1 OBJECTIVE **3**

2 BACKGROUND **3**

2.1 Gas Turbines and Microgrid Resilience 3
2.2 Prior Work with Hydrogen Blending and the C65 Engine 5
2.3 The Role of Fuel air Mixing on NOx Emissions 7

3 OBJECTIVE **8**

4 APPROACH **8**

5 METHODS/FACILITIES **9**

5.1 Test Facility Upgrades 9
5.2 Mixing Test Rig 9
5.3 Chemical Reactor Network 10
5.3.1 Reaction Mechanisms. *12*
5.3.2 Sensitivity Analysis. *13*
5.4 Engine Testing 13
5.4.1 Capstone C65 Microturbine *13*
5.4.2 Emissions *13*
5.4.3 Conversion from PPM to ng/J. *14*

6 RESULTS **14**

6.1 Mixing Studies 14
6.1.1 Velocity Field. *15*
6.1.2 Concentration Field. *15*
6.2 Engine Tests 16
6.3 NOx Inference from Mixing Studies 17
6.3.1 Natural Gas Injectors/Natural Gas Liner *19*
6.3.2 Hydrogen Injectors *20*
6.4 Extended Injector Mixing Studies 24

7 TECHNOECONOMIC ANALYSIS **27**

8 SUMMARY AND RECOMMENDATIONS **29**

8.1 Summary 29
8.2 Recommendations 29

9 REFERENCES **30**

FIGURES

Figure 1. C65 Microturbine Crossection [20] 4
Figure 2. Fuel Injector, OEM natural gas C65 Injector [2] 5
Figure 3. NOx Change relative to NG with 1175 F Turbine Exit Temperature (baseline). 5
Figure 4. Fuel Injectors for C65 Engine. 6
Figure 5. Connection between Injector Fuel/Air mixing and NOx emissions for various flame temperatures. Adapted from [28] 7
Figure 6. Schematic of C65 Combustor 10
Figure 7. Single Injector Mixing Test Rig 10
Figure 8. Chemical Reactor for C65 Combustor [33] 11
Figure 9. Horiba PG-350 Gas Analyzer [43] 14
Figure 10. Injector Exit Velocity Map. 15
Figure 11. Injector Fuel Concentration Map 16
Figure 12. Full load average NOx emissions using hydrogen injectors compared with natural gas injectors used with natural gas liner 16
Figure 13. NOx Performance vs Load for Hydrogen Injectors with LPG liner and 100% Hydrogen 17
Figure 14. NOx Emissions vs. Equivalence Ratio 18
Figure 15. Injector Exit Plane Fuel Concentration Distribution. 19
Figure 16. Flow Chart illustrating the NOx Inference process for the Engine. 19
Figure 17. Comparison of Measured and Inferred NOx 23
Figure 18. Predicted NOx Emissions vs Estimated Injector Equivalence Ratios 24
Figure 19. Baseline Injector and Extended Injector Configurations 24
Figure 20. Velocity Field at Exit Plane. 25
Figure 21. Concentration Measurements at Exit Plane. 25
Figure 22. Distribution of Equivalence Ratios Measured at the Exit Plane of the Different Injector Configruations Studied. 26
Figure 23. Summary of Full Load NOx Results (Measured and Predicted). 27

TABLES

Table 1. CRN Parameters for Each Individual Block 11
Table 2. Mechanisms Used for Each Fuel 12
Table 3. Details Regarding Mechanisms Used 12
Table 4. Predicted NOx Emissions based on Measured NG injector concentration data and “Perfect Mixing” Compared to Measured NOx Emissions 20
Table 5. Predicted NOx Emissions based on Measured Hydrogen Injector concentration data and “Perfect Mixing” Compared to Measured NOx Emissions for Natural Gas Operating Condition 21
Table 6. Equivalence Ratio prediction based on emissions using hydrogen injectors and NG Liner 21
Table 7. Equivalence Ratio prediction based on emissions using hydrogen injectors and LPG Liner 22
Table 8. Equivalence ratio prediction considering 1/5 flame size for hydrogen compared to NG with LPG liner 23
Table 9. Relative GHG and Pollutant Emissions for Hydrogen Fueled Engine vs Natural Gas Fired Engine. 28

EXECUTIVE SUMMARY

This project builds upon work done previously under Agreement 5660055707 which was focused on extending the Capstone C65 and C200 microturbines towards operation on up to 30% hydrogen blended into natural gas. The current effort, in cooperation with Capstone Green Energy, pushed the operation of the C65 to 100% hydrogen and worked on minimizing NOx emissions. While natural gas injectors were capable of operation on up to 30% hydrogen, they would flashback with higher levels. As a result, Capstone provided fuel injectors specifically designed for operation on hydrogen which requires consideration for operability challenges such as flashback when operated with premixing which is desired for low emissions. The effort demonstrated operation of the engine on 100% hydrogen from cold start to full load without any operability issues noted. Yet the NOx emissions were higher than desired at about 180 ppm. To address this, working with Capstone, the combustor liner was changed from one designed for operation on natural gas to one designed to work with liquid petroleum gas (LPG). Further, additional instrumentation for monitoring fuel flow and electricity generated was added along with upgrades to the facility fuel system to meet NFPA and ASME standards for hydrogen. The LPG liner forces more air to the injector which helps reduce the chance of flashback even for a fuel like LPG which is more reactive than natural gas and leans out the fuel/air mixture which reduces combustion temperature and NOx.

The use of the hydrogen injectors with the LPG liner demonstrated that a 24% reduction in NOx could be attained. Several rounds of emissions measurements with the hydrogen injectors and LPG liner showed good repeatability. In addition, under the current effort, emissions were measured as a function of engine load to help elucidate how NOx changes with output power.

In the current effort, the well-established connection between mixing performance and NOx emissions was studied to help understand the reasons for the elevated NOx emissions when compared to operation on natural gas. When compared to established “NOx entitlement” levels, the C65 engine operated on natural gas is found to attain the lowest expected NOx emissions for a given flame temperature. This was presumed to be a result of injector mixing performance. To study mixing performance, a fuel injector mixing test rig was established and used to quantify the mixing performance of the natural gas and hydrogen injectors. The results showed that the mixing for the hydrogen injectors was less effective than for the natural gas injectors. The natural gas injectors demonstrated very good mixing, consistent with the very low NOx emissions levels produced by the engine.

In addition to the mixing rig, a simulation approach using chemical reactor networks (CRN) was established. This tool was further enhanced by incorporating a strategy to account for imperfect mixing from the injector. The CRN was also adapted to be used for both natural gas and hydrogen. Using the CRN, predicted NOx emissions levels were able to match measured levels from the engine for both natural gas and hydrogen. As a first step to demonstrate how injector geometry might impact emissions, a 1-inch extension was added to the original hydrogen injector and the mixing performance measured. The modest modification resulted in improved mixing performance. The CRN was used to estimate the impact of this change on NOx and it was found that NOx levels may reduce by 39%. Furthermore, the CRN was used to estimate the NOx emissions if perfect mixing could be attained with the injector and this suggested about 10 ppm NOx could be attained, approaching the same levels as natural gas. Figure ES-1 summarizes the NOx emissions observed and predicted under this study.

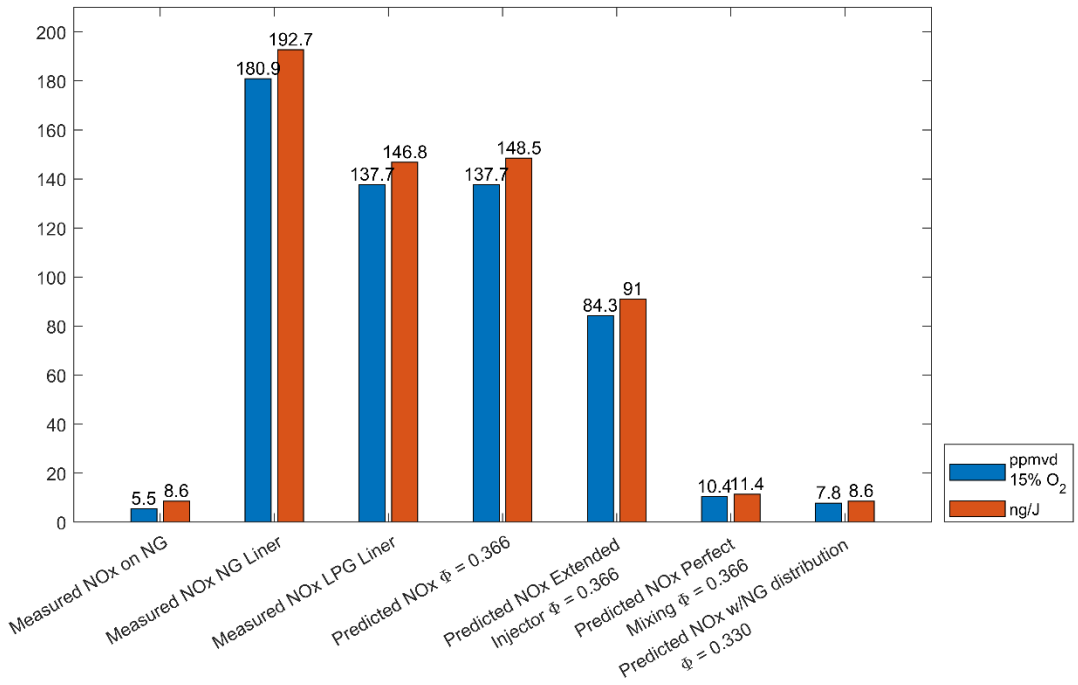

Figure ES-1. Summary of Measured and Predicted NOx results for C65 operated on 100% Hydrogen at Full Load.

The results show that shifting air around the engine combustion system should result in NOx levels comparable to natural gas. Hypothetically, NOx emissions on hydrogen can equal or be less than the NOx emissions from the CARB certified commercial C65 engine operated on natural gas.

The next steps are to fabricate a set of extended injectors (which will improve mixing) and test them in the engine to confirm the results of the CRN. From that point, further modifications could be considered, including additional liner configurations, further improving the mixing performance of the injectors, changing the injector fuel staging points, and varying the turbine exit temperature set point. In parallel, computational fluid dynamics (CFD) can be considered to help develop injector designs in a systematic fashion (e.g., using statistically designed parametric studies) that can improve mixing performance. Select configurations can be built and the resulting mixing performance assessed. Promising configurations can then be fabricated and tested in the engine.

1 OBJECTIVE

The objective of this effort is to leverage existing work done to retrofit a commercial microturbine to operate on up to 100% hydrogen by volume while at the same time achieving NOx emissions levels on par with the existing commercial natural gas fueled levels. It is desired to understand how various parameters can be modified to impact NOx emissions. Of particular interest are the fuel injector mixing effectiveness and the combination of fuel injector and combustion liner open areas to distribute air to various regions in the combustor. Further, the role of readily changeable engine control parameters such as turbine exit temperatures (TET) are also of interest. The overall goal is a field retrofittable solution to attain a low emission gas turbine generator capable of operating on pure hydrogen. This would pave the way for deployment as a dispatchable power source as part of a hydrogen microgrid.

2 BACKGROUND

2.1 Gas Turbines and Microgrid Resilience

Microturbine generators (MTG) offer a compact option for dispatchable power generation that is well suited for microgrids and integration into a diverse system involving renewable energy, storage, heating and power requirements, and economic dispatch [1,2,3]. Recently, the concept of using hydrogen to decarbonize the natural gas system or as a local decarbonization strategy within a microgrid is gaining increased interest [4]. In this context, the dispatchable system, such as an MTG, must exhibit a degree of fuel flexibility to accommodate hydrogen as a fuel. A key performance factor, especially for a microgrid application, is the impact of adding hydrogen on pollutant emissions. When used in a microgrid configuration, proximity to population will be more likely and thus a reduction of NOx to minimize local ozone and particulate formation is important to protect health. Microturbine generators have already demonstrated low single digit NOx emissions and, in some cases, have attained certifications levels that indicate performance on par with the cleanest, highest efficiency central station power plants [5], including the engine under consideration in the present study. This means NOx emissions are below 0.07 lb/MW-hr (which translates into low single digit NOx levels on a ppmvd @ 15% O_2 basis). This engine relies on well-established lean premixed operation combined with heat recuperation to attain this impressive emissions performance. Heat recuperation is associated with using a heat exchanger to transfer heat from the exhaust into the air fed to the combustor by the compressor. This heat transfer increases the efficiency of the thermodynamic cycle but also increases the temperature of the air fed to the combustor.

When considering the use of hydrogen in a recuperated microturbine operating in a premixed combustion mode to attain low emissions, several factors must be considered regarding the characteristics of hydrogen [6]. Of particular interest are the high flame speed of hydrogen and the relatively low ignition energy required. Regarding autoignition, studies have suggested that, even with the higher combustor inlet temperature associated with the recuperated cycle, with a reasonable aerodynamic design for the premixer, substantial margin for avoiding autoignition exists [7]. As a result, the principal area of concern is often flashback [8].

The use of hydrogen in small, recuperated engine configurations has been the subject of several studies. In many cases, these are focused on what was the Turbec T-100 engine which features a can combustor architecture and is currently offered by Ansaldo Energia (AE-T100). The

majority of these studies have emphasized numerical simulations [9,10,11,12]. Some experimental efforts have also been directed at combustor configurations operated outside of the engine with purpose of modifying the baseline configuration to adapt hydrogen addition [13,14]. These studies indicated that the combustor configuration could be adapted for hydrogen and maintain good operability. One numerical study suggested operation on 100% hydrogen could be attained with NOx emissions below those of natural gas [10]. In terms of emissions, one study on a combustor modified to implement the flameless oxidation (FLOX® [15,16]) combustion regime found that NOx values, while increasing slightly (from 2 to 4 ppm) as hydrogen addition was increased from 0 to 30% [14], remained quite low.

The other architecture studied is a staged, annular, tangentially fired arrangement as illustrated in Figure 1. This is the configuration offered commercially by Capstone Green Energy Corporation in their microturbines. A handful of studies have been carried out in an actual engine (e.g., a 60kW engine was studied in [17]). Experimental studies have been carried out using combustion configurations operated external to the engine to generate understanding of the behavior of the combustion when hydrogen is added [18,19]. In these studies, low single digit NOx levels were demonstrated for natural gas operation, but NOx levels increased as hydrogen levels exceeded 50%.

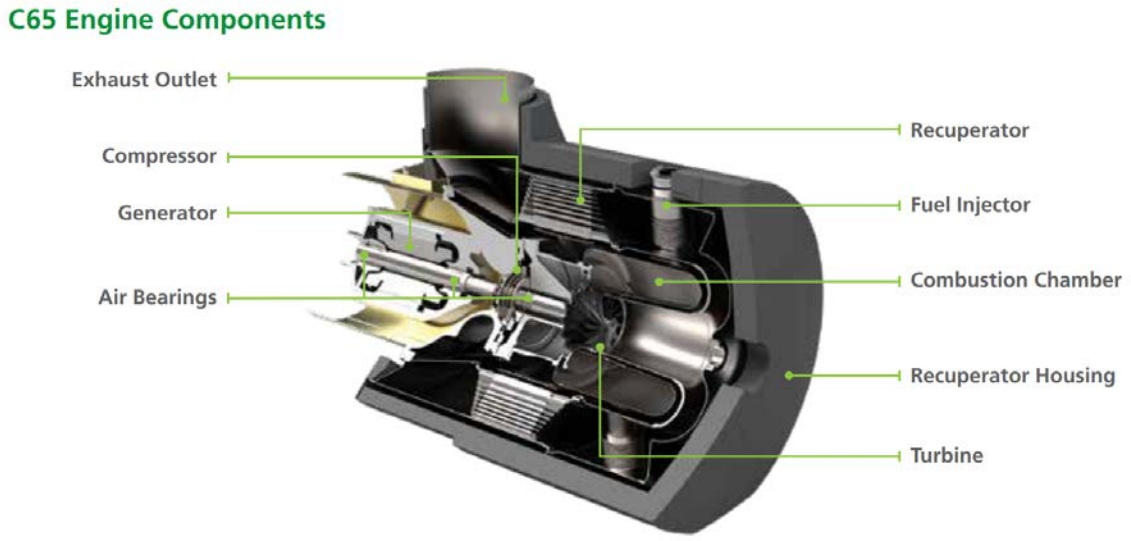

Figure 1. C65 Microturbine Crossection [20]

The studies in both combustor configurations suggest that some level of hydrogen can be accommodated in these premixed systems. Emissions can be tempered by taking advantage of the diluent mixing process. This appears especially true with the implementation of FLOX® technology. It is evident that the combustion behavior changes significantly when the volume percentage of hydrogen in the fuel exceeds 75% [17,18].

For the configuration studied in the present effort, featuring non-swirling jet like fuel injectors, application of a previously developed flashback correlation [21] suggests that up to 30% hydrogen could be tolerated in the fuel injector. The correlation was derived from studies of an isolated fuel injector in a high-pressure test rig, not in an actual engine. Hence, while the correlation suggests tolerance to up to 30% hydrogen numerous questions remain regarding the application in the engine. It is noted that the combustor configured for FLOX® combustion strategies also exhibited no signs of flashback at up to 30% hydrogen in the [14].

2.2 Prior Work with Hydrogen Blending and the C65 Engine

Previous work with Southern California Gas (Agreement 5660055707) and Capstone Green Energy demonstrated operation of the natural gas engine on up to 20% hydrogen. The goal of this work was to understand if the commercial C65 engine configured for natural gas could operate over the full range of loads (including start and stop) on up to 20% hydrogen using combustion liners, injectors, and fuel control systems meant for natural gas. The normal OEM fuel injector for natural gas is shown in Figure 2. Based on discussions with Capstone regarding expected upper limits on hydrogen, the upper limit for the overall study was pushed to 30% hydrogen.

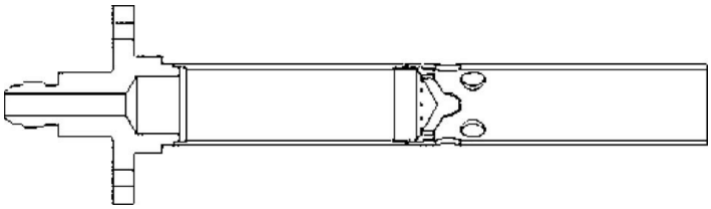

Figure 2. Fuel Injector, OEM natural gas C65 Injector [2]

This prior effort was successful in that it demonstrated 1) the engine could operate on up to 30% hydrogen without any modifications and 2) an understanding of how hydrogen content and turbine exit temperature (a settable parameter on the engine) impacted NOx relative to natural gas operation. An example of the NOx behavior from this prior work is summarized in Figure 3 which illustrates that NOx levels increase as hydrogen is added and as Turbine Exit Temperature set point is increased. A key corollary observation is that the engine can attain NOx levels equivalent to those for natural gas (i.e., Delta NOx =- 0 ppm) by lowering the turbine exit temperature to 1160 F. No discernable engine output derate was observed when changing the set point from 1175 F to 1160 F. Furthermore, CO was reduced substantially when operated on 20% hydrogen blended into natural gas, as expected.

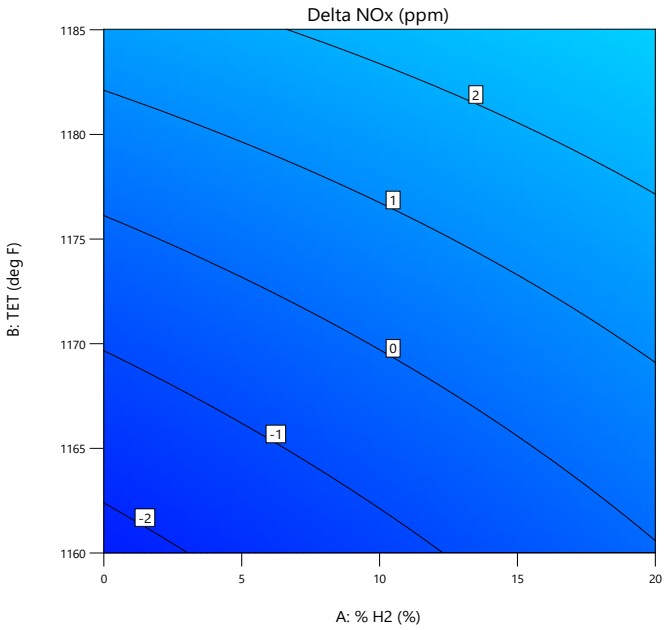

Figure 3. NOx Change relative to NG with 1175 F Turbine Exit Temperature (baseline).

For context, the Capstone C65 natural gas unit is rated for NOx emissions below 9 ppmvd @ 15% O2. Measured values previously and for the current effort on natural gas are typically 4-6 ppm. Hence, an initial target performance for operation on hydrogen blends is to maintain NOx levels below 9 ppm. Hence the results shown in Figure 3 indicates that typical NOx levels, even with 20% hydrogen at the nominal turbine exit temperature, will remain below 9 ppmvd @ 15% O2. The result in Figure 3 suggest an increase of less than 2 ppm, which given the typical natural gas results of 4-6 ppm will still be below 9 ppm.

As a result of this prior work and work with Capstone, warranted operation of the C65 and C200 engines on up to 30% hydrogen blended into natural gas is available to customers [23].

In parallel with the work to guarantee performance of commercial equipment on up to 30% hydrogen, other work has been conducted to design/evolve fuel injectors for the Capstone C65 engine that are capable of injecting 100% hydrogen as a fuel. An initial design of an injector to avoid flashback was tested at UC Irvine in its high-pressure test rig. The design of the flashback resistant injector [24] is shown in Figure 4b in comparison to the commercial engine natural gas injector shown in Figure 4a.

Key features associated with the design for hydrogen include (1) more air addition by the injector resulting in leaner overall mixtures and higher velocities, (2) injection of air along the wall of the final length to further lean out the mixture near the wall and (3) reduced residence time to avoid possible auto ignition concerns. These design features directly address flashback pathways along the boundary layer and in the core flow. It also addresses emissions by leaning out the fuel-air mixture . The design has facilitated operation on 100% H_2 without flashback in the UCI high pressure test rig and is therefore a critical success [25].

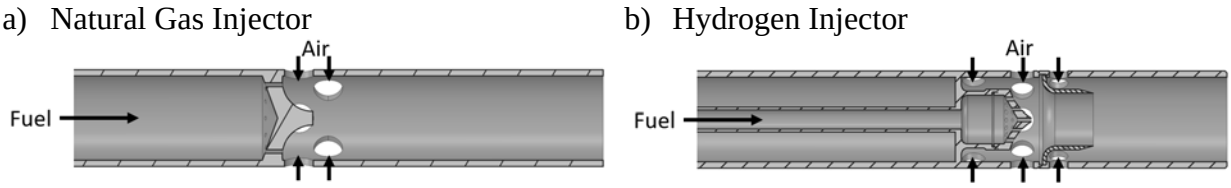

Figure 4. Fuel Injectors for C65 Engine.

The next steps taken with support from Capstone was to test a set of the injectors shown in Figure 4b in the engine. These tests pushed the envelope of the current test facilities which were not really designed for operation on 100% hydrogen. But with the limited testing to be done along with the outdoor nature of the test setup, a decision was made to run these quick tests to validate if the injectors could allow engine operation on 100% hydrogen. These tests were carried out using a natural gas liner as an initial baseline. Results were obtained for full power and demonstrated that the engine could be started on hydrogen and ramp up and down in load without any operability issues. This was a major milestone, representing the first time a C65 engine had been operated on 100% hydrogen from cold start to full load. While the hydrogen injector did facilitate successful operation on hydrogen, the measured NOx levels with this configuration was 181.4 ppmvd @ 15%O2. This corresponds to 193.2 ng/J. These levels were well above the target level of 9 ppmvd @ 15% O2. The reason for the elevated NOx was not completely evident. In consideration of the role of mixing discussed in the next section, one hypothesis is that the mixing performance is not sufficient. Alternatively, it could be that the global mixing behavior with the more compact hydrogen reaction may play a role.

Despite the major milestone of attaining flashback free operation on 100% hydrogen in the test rig and in the engine, the NOx performance was far from desirable. This leads to a need to make

modifications to improve performance. As part of this, understanding the actual fuel/air mixing performance of the injectors is critical to understand why the NOx levels are elevated. With mixing levels quantified, strategies for improving performance can be postulated. The next section provides background and context as to why understanding mixing performance is critical to the evolution of the injector design to attain low NOx emissions.

2.3 The Role of Fuel air Mixing on NOx Emissions.

Because of the importance of NOx emissions in the South Coast Air Basin, it is critical that any shift toward low or zero carbon fuels must also be accompanied by maintaining or reducing NOx emissions. As shown above in Figure 3, at up to 30% hydrogen blending, the NOx levels are minimally affected and can be controlled readily by making software setting changes (e.g., slightly lower turbine exit temperature set point). But this is with a system that has been evolved specifically for low emissions over a couple of decades by Capstone. As mentioned above, the C65 is one of the engines that is CARB certified for NOx emissions [5]. A key reason it can attain such low emissions on the natural gas is that the fuel and air are well mixed prior to the injection into the combustion chamber.

It has been well established that the mixing performance of fuel injectors can greatly impact NOx emissions from lean premixed gas turbines. Fundamental work by Lyons and Fric [26,27] established a strong connection between fuel air mixing and the resultant NOx from combustion of the mixture. Further, Leonard and Stegmeier (1994) set a framework that directly associates NOx emissions with various levels of premixing attained [28]. Leonard and Stegmeier took the work to the point of establishing an "entitlement plot" to reflect the expected "minimum NOx" emissions that could be expected for natural gas and air combustion for gas turbines as a function of the reaction temperature (established as the adiabatic flame temperature (see Figure 5). This work helped guide the development of low emissions gas turbine combustion systems. Extensive work has been carried out on the Capstone C65 engine to optimize its emissions performance on natural gas. Figure 5 includes a measured NOx emissions point for the Capstone C65 engine and it infers the mixing is essentially optimized. Thus, the fact that the C65 engine is CARB certified is testimony to the maturity and optimization of the fuel air mixing for this system.

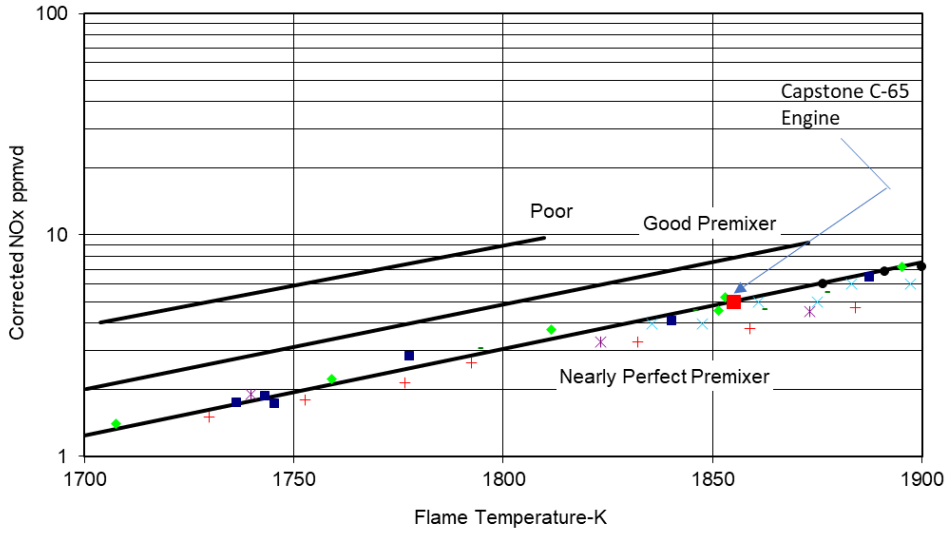

Figure 5. Connection between Injector Fuel/Air mixing and NOx emissions for various flame temperatures. Adapted from [28]

Relative to applying the same entitlement concept to other fuels, recent work has shown some challenges with the reporting basis especially when hydrogen is considered. Reporting NOx emissions on a ppmvd basis creates an inherent bias that increases apparent NOx levels for hydrogen because of the relatively high amount of water generated as a function of fuel type [29,30]. Hydrogen combustion creates more water in the exhaust than does natural gas for a given fuel/air mixture. As a result, when the sample is dried as part of the sample preparation step for introduction into the emission analyzer, the remaining species increase in concentration for the hydrogen case. As a result, pure hydrogen combustion results in about 35-40% higher ppm levels of species such as NOx compared to natural gas combustion because of this effect. Essentially, the same mass emission of NOx (e.g, ng/J) translates into a concentration-based emission level (i.e., ppmvd @ 15% O_2) that is 35-40% higher for hydrogen than it is for natural gas. As a result of this bias, for example, Figure 5 is truly only valid for natural gas. Yet similar efforts for aeroengines utilized a mass emission basis which is valid regardless of the fuel type [31]. As a result, work done on optimization of mixing and the associated NOx emissions requires further effort to establish target limits.

Reflecting again upon the high NOx levels for the hydrogen injectors, in light of the above discussion on mixing and NOx, a key question is: what is the mixing performance of the hydrogen injectors compared to that of the low NOx natural gas injectors? In the absence of information on the injector mixing performance, it is not known what the mechanism is for the elevated NOx.

3 OBJECTIVE

While previous work has established that the microturbine can be successfully operated on up to 100% hydrogen, generally with some level of modification, the objective of the current work is to move to operation of the engine on 100% hydrogen while minimizing NOx emissions. While the flashback resistant injector design proved promising to attain flashback free engine operation, systematic data on emissions have not been obtained. Furthermore, no information on injector mixing performance has been provided. As a result, the objectives of the current study are (1) quantify the mixing performance of the injector, (2) establish a tool to connect mixing performance to emissions performance, and (3) safely operate the C65 engine on 100% hydrogen by adhering to safety codes and standards.

The rationale for objective 2 is twofold. First, testing with 100% hydrogen is expensive and secondly, fabricating a set of 6 injectors to carry out engine tests is also expensive. Furthermore, because mixing performance is clearly connected to NOx emissions, a way to infer NOx performance based on measured emissions for a single injector (one that could be made using lower cost materials that an engine injector) would allow a time efficient, lower cost approach to minimizing emissions.

4 APPROACH

The approach in the current effort consisted of 5 Tasks:

- Task 1: Prepare the test facilities and test engine for 100% hydrogen. This task consists of modifying the piping systems to operate leak free on 100% hydrogen following ASME codes. In addition, fuel injectors to operate without flashback needed to be procured.

- Task 2: To guide design of injectors, quantify the mixing performance of the baseline natural gas injectors and the initial hydrogen injectors
- Task 3: Establish and validate CFD/Reactor Network analysis to guide injector design
- Task 4: Engine Testing
- Task 5: Technoeconomic Analysis

In the following sections, information is presented on the facilities and methods which are involved in Tasks 1-4. Following that results are presented along with limited technoeconmic analysis which is Task 5.

5 METHODS/FACILITIES

5.1 Test Facility Upgrades

As part of Task 1, upgrades to the C65 piping were made to exercise safety and comply with NFPA 2 and ASME B31.12 safety standards and codes for hydrogen. The pipe upgrades were mainly done based on the ASME B31.12 standard as NFPA referenced it on theirs. ASME B31.12 is specific to hydrogen piping and pipelines and thus was the code that was mainly followed. The piping material was changed to 316 stainless steel because irons are prohibited, per B31.12 GR-2.1.4, due to their lack of ductility and sensitivity to thermal and mechanical shock. Almost all the joints use compression type fittings with a couple of exceptions: gas cylinder regulators, pressure gauges, and a solenoid valve used for an emergency stop, all of which use general purpose taper pipe threads (NPT). These exceptions are permitted under ASME B31.12 IP-5.5.1 which states that taper threaded joints may be used on systems at operating pressures under 3,000 psig. The piping system for the C65 operates at 150 psig at most, therefore, it is well below the limit stated by ASME B31.12. A new Coriolis flow meter with compression fittings was installed because the old meter used flanged connections. A vent that extends over 10 ft above the turbine inlet was also included in the piping. Lastly, NFPA 2 7.2.2.3.2.4 Air Intakes states that storage and use of GH_2 cannot be located within 20 ft of air intakes. The turbine was moved so that it would be 20 ft away from the fuel source.

Multiple leak tests were performed using snoop after the installation of the new piping system was completed. The piping system was filled with natural gas to detect leaks as an initial test. The system was vented to rectify the and the process was repeated a second time. The system was again vented, and the leak test was performed using hydrogen. The test was repeated with hydrogen until leaks were no longer detected. A pressure test was performed afterward to verify that the piping system would maintain pressure for 1 hour.

5.2 Mixing Test Rig

In the present study, a single injector mixing rig was developed as part of Task 2 to mimic the flow conditions about the injector. The annular arrangement and integrated recuperator associated with the C65 combustor creates a somewhat complex flow pattern around the injector which has been shown previously to affect the distribution of velocity and concentration at the exit of the injector [32]. The staging arrangement and fuel/air injection strategy is illustrated in Figure 6 and Figure 7. The rightmost image in Figure 7 shows the actual injector mixing rig used. To quantify mixing, natural gas was injected and the exit of the injector (approximately 25 mm) was mapped out using a 1.6 mm o.d., needle which pulled a gas sample to a flame ionization detector (Horiba

FIA 220) which measured the concentration of natural gas in the mixture. In addition, the velocity of the exit plane was also documented using a 3.175 mm diameter pitot probe. The injector was positioned precisely using a 3D optical encoder (Mitutoyo) and digital readout. Positioning is precise to ~0.5 mm.

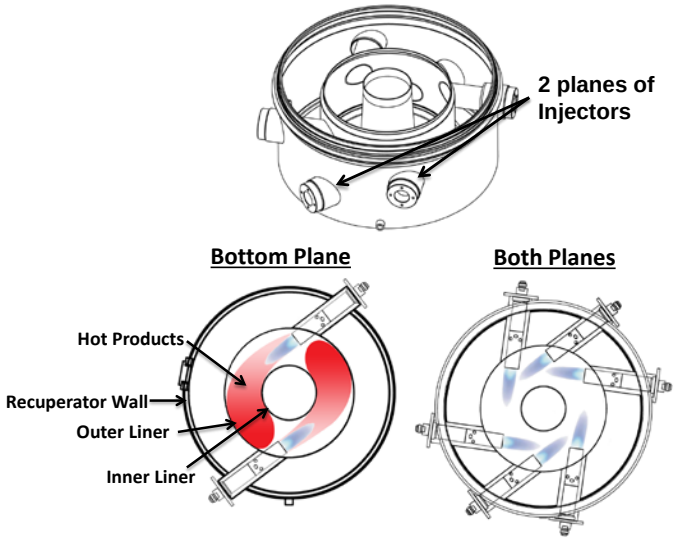

Figure 6. Schematic of C65 Combustor

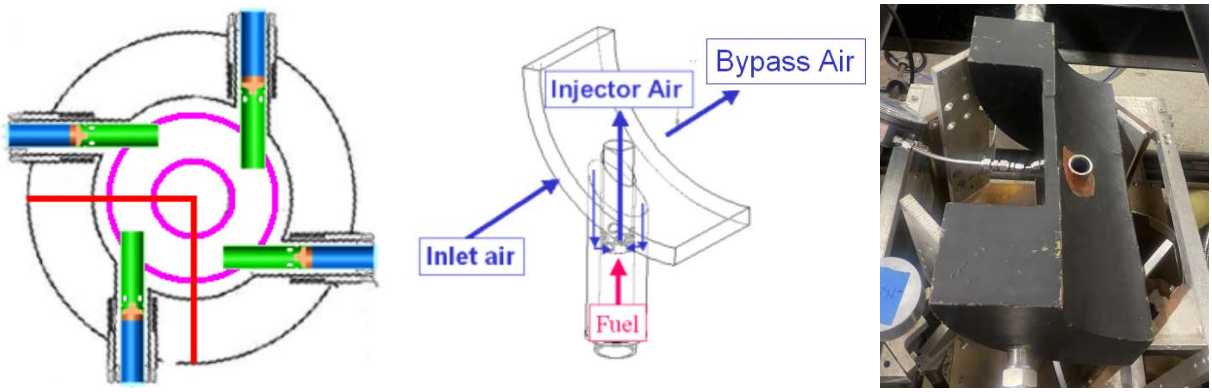

Figure 7. Single Injector Mixing Test Rig

5.3 Chemical Reactor Network

A chemical reactor network (CRN) was established to connect the mixing behavior to expected emissions as discussed in Section 1. This network was conceptualized and validated for the C65 in previous work that examined how added higher hydrocarbons as well as hydrogen impacted performance [33]. Pure hydrogen was not studied in prior work which is noteworthy in terms of assumptions regarding reactor volumes for the present work. The CRN is composed of different zones that are intended to simulate characteristics of the combustion process in the engine. It consists of 8 PSR's 1 Gas Mixer, 2 Gas Splitters, and 2 Gas inlets. It accounts for the geometric volume of the combustor, as well as variables such as pressure and temperature. The premixed air passes from the gas mixer into the first gas splitter, which simulates the gas entering two planes of injectors. The second gas splitter is used to simulate recirculation of the exhaust from the first plane of injectors entering the second plane of injectors. The second inlet is used to simulate the dilution of the products with air near the exhaust of the combustor.

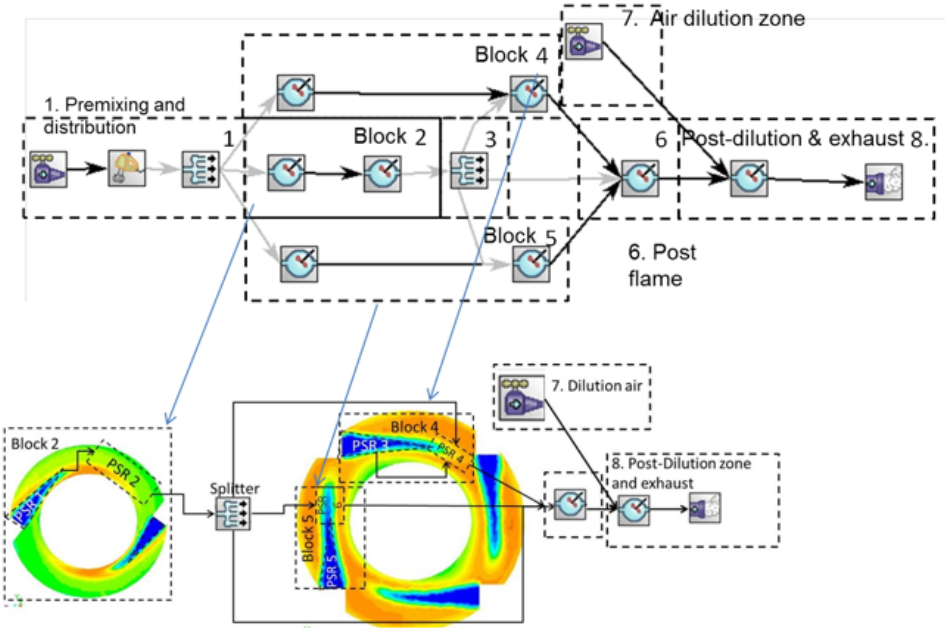

Figure 8. Chemical Reactor for C65 Combustor [33]

The parameters for each individual section in the CRN are based on CFD results [33] and are listed in Table 1. For the present work, volumes were adjusted based on ratio of flame speeds for natural gas and hydrogen which was estimated to be about a factor 3-7.

Table 1. CRN Parameters for Each Individual Block

Model:	Temperature:	Pressure:	Flow Rate:	Split:	Volume:
I1	833K	N/A	148.81 g/sec	N/A	N/A
M	833K	4.2 atm	N/A	N/A	N/A
S1	N/A	N/A	N/A	0.34 to PSR1, 0.33 to PSR3 and PSR5	N/A
PSR1	833K	4.2 atm	N/A	N/A	75.5 cm^3
PSR2	1812K	4.2 atm	N/A	N/A	90 cm^3
S2	N/A	N/A	N/A	0.86 to PSR7, 0.07 to PSR4 and PSR6	N/A
PSR3	833K	4.2 atm	N/A	N/A	75.5 cm^3
PSR4	1812K	4.2 atm	N/A	N/A	90 cm^3
PSR5	833K	4.2 atm	N/A	N/A	75.5 cm^3
PSR6	1812K	4.2 atm	N/A	N/A	100 cm^3
PSR7	1812K	4.2 atm	N/A	N/A	100 cm^3
I2	650°F	N/A	235 g/sec	N/A	N/A
PSR8	1812K	4.2 atm	N/A	N/A	990 cm^3

5.3.1 Reaction Mechanisms.

Underlying the NOx calculations, a detailed kinetic mechanism is needed that can elucidate the complex fuel oxidation process. Several reaction mechanisms were tested for the 100% CH_4 case and 100% H_2 case. The mechanisms initially tested were Ansys H_2, 34 Grimech 3.0 [35], Galway-Syngas (2017) [36], Konnov v0.5 [37], and UCSD Combustion Mechanism (2016) [38]. Aramcomech 3.0 was included as it is a generalized mechanism that contains 1140 species [39]. However, it does not contain NOx chemistry. For use in this project, the Aramco mechanism was modified by UC Irvine to obtain NOx emissions by incorporating the NOx chemistry data from the Ansys mechanism. The HyChem mechanism [40] was also included in the study as recent studies have suggested it is a useful mechanism for use mixtures of hydrogen and natural gas [41] and also includes a recently updated NOx mechanism from Glarborg [42]. The Galway-Syngas 2017 and Ansys H_2 mechanisms were used only in cases involving 100% H_2 as they do not have CH_4 chemistry. Table 2 summarizes the mechanisms that were used for each fuel. Table 3 provides some details regarding each mechanism.

Table 2. Mechanisms Used for Each Fuel

Fuel	Mechanisms				
CH_4	Grimech 3.0 (1999)	Konnov v0.5 (2007)	UCSD (2016)	Aramcomech 3.0 (2020)	HyChem
H_2	Galway-Syngas (2017)	Ansys H_2	Aramcomech 3.0 (2020)	HyChem (	

Table 3. Details Regarding Mechanisms Used

Mechanism	Species	Reactions	Comments
GRIMech (1999)	53	325	-Common mechanism for hydrocarbons. -Optimized for high temperature methane -NOx chemistry included. -Not suitable for pure hydrogen
Konnov v0.5 (2007)	127	1200	--Optimized for small hydrocarbons -NOx chemistry included -Not suitable for pure hydrogen
ANSYS H2 (2009)	21		--Not suitable for methane --NOx chemistry included
UCSD (2016)	57	268	-Not suitable for pure hydrogen
Galway Syngas/NOx (2017)	44	54	-NOx chemistry included -Not suitable for methane
AramcoMech 3.0 (2020)	1140		--NOx chemistry from ANSYS H2 added "ad hoc" by UC Irvine as part of this study
HyChem (2019)	81	1367	--A2/C1 blend --NOx chemistry included

To facilitate comparison between natural gas and hydrogen, it was desired to utilize one mechanism for both cases. This may not be an optimal approach as it is evident that some mechanisms have been optimized specifically for natural gas and therefore might be preferred for that fuel. That said, only AramcoMech and HyChem mechanisms worked well with both natural

gas and hydrogen. However, because The ANSYS H2 NOx chemistry was added in an "ad-hoc" manner to AramcoMech, it was felt that this approach may not be deemed rigorous compared to an overall optimized mechanism including NOx chemistry in the development process. As a result, in the present effort, the focus was on HyChem. Regardless, sensitivity studies (Section 5.3.2 below) were carried out to help illustrate the sensitivity of the results to the mechanism used. Interestingly, the other mechanisms that worked with natural gas predict unreasonably low NOx values for hydrogen (low single digit values compared to higher values for natural gas when compared at the same equivalence ratio and flame size). As a result, these were deemphasized.

5.3.2 Sensitivity Analysis.

A sensitivity study in which the reaction mechanisms were varied was conducted to determine which mechanism matched experimental data best. The 5 reaction mechanisms discussed above were also used in the CH_4 study to show the differences that arise because of different NOx calculation formulas. It was observed that the reactor temperature (see Table 1) did not have a significant impact on NOx emissions.

5.4 Engine Testing

5.4.1 Capstone C65 Microturbine

The Capstone C65 Microturbine is a multi-fuel turbine capable of producing up to 65kW of power generation. The C65 has six fuel injectors arrayed in two stages creating a primary combustion zone between the two stages. The first stage has two fuel injectors with the other four injectors in the second stage. Air comes in through the intake and is sent through the compressor. After the compressor, air is sent through the recuperator and to the combustion chamber and two dilution zones [17].

For the present study, two combustion liners are used. The first is the standard natural gas liner. The second is a liner used for LPG. The LPG liner has a set of blocked dilution jet holes which "forces" more air into the injector thus leaning out the combustion zone and reducing combustion temperatures. As a result, there are four combinations of engine test hardware that can be tested which include the two injectors (Figure 4) and these two liners. The leanest overall mixture would be attained with the hydrogen injectors paired with the LPG liner. It is also possible to vary the turbine exit temperature as well in order to affect the NOx performance as illustrated in the previous SCG project.

5.4.2 Emissions

Emissions are measured using a Horiba PG-350 analyzer. PG series are portable gas analyzers that measure common criteria air pollutants NOx, CO, SO_2 as well as CO_2 and O_2. The gas analyzers use fluid modulation chemiluminescence (CLA-NO) analyzer, fluid modulation infrared Absorption analyzer (CO, SO_2), Light Source Modulation Infrared Absorption Analyzer (CO_2), and Zirconia Oxygen Analyzer (O_2). The PG-350 analyzer can measure NO_x using a separate testing circuit which can measure all NO_x variants beyond just NO of the more basic PG-235 [43]. The stated accuracy is 1% of full scale, thus the measurement accuracy is ±0.25 ppm for NOx, ±1ppm for CO, and ±0.25% for O_2. The analyzer was zeroed and spanned using span gases at about 80% of the full-scale range used. This was done before and after each test run and generally exhibited drift of less than 1% of the readings. The sample was conveyed to a refrigerated water drop out system via a 5 meter 6 mm Teflon line prior to entry into the analyzer. No evidence of condensation in the line prior to the water dropout system was noted. No attempt was made to account for cross species interferences. Based on the expected concentrations of the main

interfering species (CO and CO_2), the interference effect on NO and CO measurements is expected to be less than 0.7% of the reading [43].

Figure 9. Horiba PG-350 Gas Analyzer [43]

5.4.3 Conversion from PPM to ng/J.

As discussed above, comparing emissions between hydrogen and natural gas on a ppmvd basis leads to an inherent bias. As a result, to circumvent this issue, emissions values are converted to a ng/J basis using Equation 1 to convert the measured ppmvd values into ng/J:

$$E = X * C * F * \frac{20.9}{20.9 - \%O2} \quad (1)$$

In Equation (1) is the oxygen based F-factor conversion method in which *E* is the converted emissions with units in ng/J. *X* is a conversion factor that converts ml/SCM to ng/SCM. *C* is the dry concentration of uncorrected emissions of interest in ppmvd, which in this case is NOx. *F* is the F factor which is based on the caloric value of the fuel being used in kJ/kg, along with the weight percentage of individual atoms that make up the fuel. Lastly, $\%O_2$ is the dry percentage of O_2 in the sample (also measured using the emissions analyzer).

6 RESULTS

In this section, the results are presented. The results start with measured fuel injector exit plane mixing performance which are then ported to the reactor network to estimate NOx emissions that result from the distribution of equivalence ratios measured. The inferred NOx results are then compared with measured results from the engine.

6.1 Mixing Studies

In this section results are presented for the velocity and concentration field at the exit plane of each injector.

6.1.1 Velocity Field.

The injector flow was set using a pressure drop similar to that expected in the engine, around 4%, which corresponds to 16-inches of water column. The bypass was established such that about 40% of the air flowed to the test rig entered the injector with the remaining about bypassing the injector. This split established the approximate flow dynamics in the engine. Using this strategy, the resulting velocity of the air exiting the injector was mapped out using the pitot probe. As shown in Figure 10a, the velocity is not symmetric for the natural gas injector. This is due to the complex flow pattern established by the bypass air flowing around the injector (recall Figure 7). The symmetry of the flow field for the high flame speed injector appears slightly superior to that of the natural gas injector. The overall velocity levels are higher for the high flame speed injector which is consistent with the design intent. In terms of overall uniformity, the natural gas injector varies by 4% over the plane with a bulk average velocity of 36.1 m/s whereas the high flame speed injector varies by 7.7% with a bulk average velocity of 43.4 m/s.

a) Natural Gas Injector b) High Flame Speed Injector

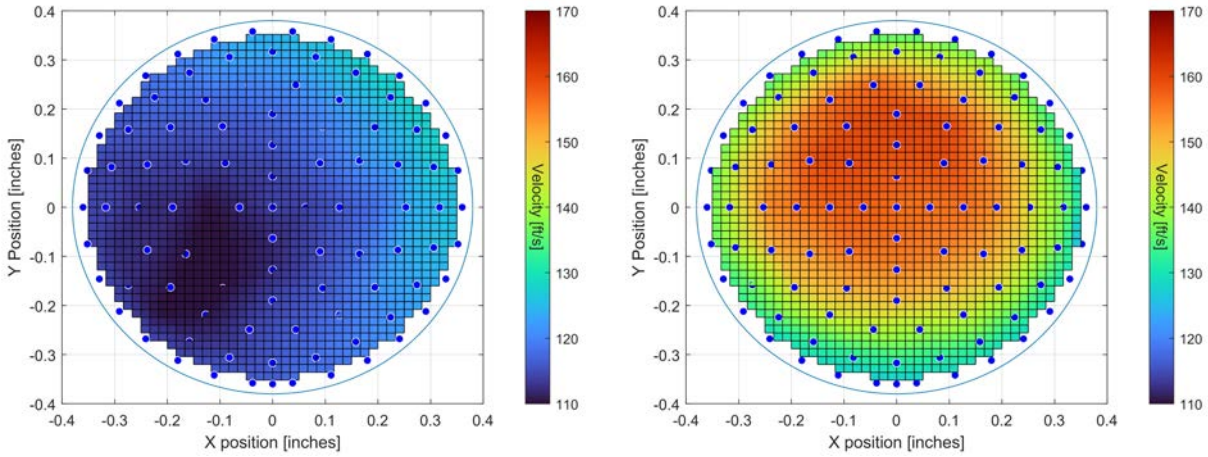

Figure 10. Injector Exit Velocity Map.

6.1.2 Concentration Field.

The corresponding fuel concentration field is shown in Figure 11. As shown, the fuel distribution is relatively uniform for the natural gas injector, whereas it has considerable variation for the high flame speed injector. The standard deviation divided by the average is 6.5% for the natural gas injector, whereas for the high flame speed injector it is 85%. This comparison is not completely fair because the low values near the wall for the high flame speed injector are intentional, a result of flowing air along the wall to help ensure boundary layer flashback does not occur. A better index for the high flame speed injector would be the uniformity over the center region of the flow formed by the venturi shown in Figure 4b, but for an initial comparison this is not considered. Regardless, with the approach taken, the outer region would not contribute to the NOx emissions as the mixture would be below the flammability limit. And the approach certainly captures the impact of the local mixing levels over the entire exit plane.

c) Natural Gas Injector d) High Flame Speed Injector

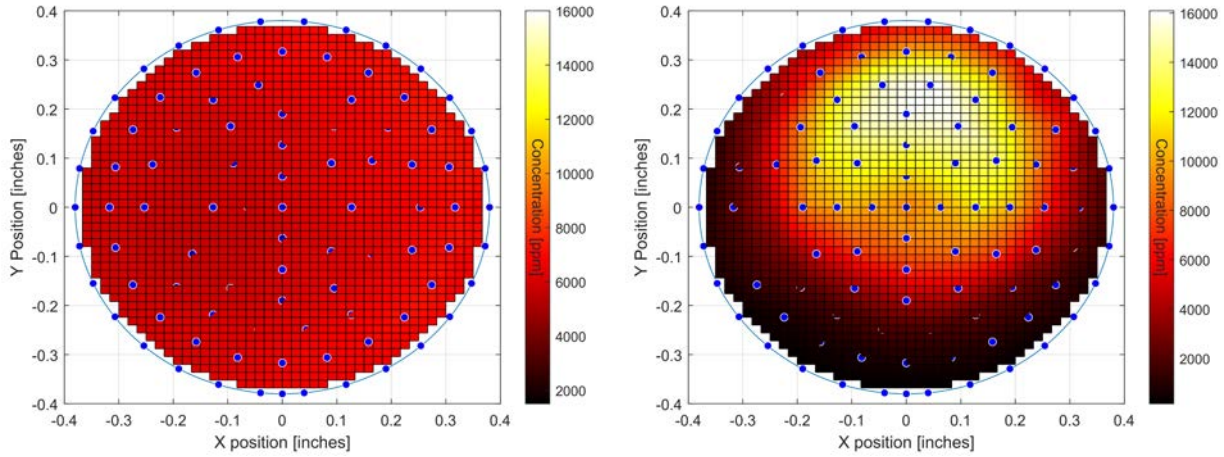

Figure 11. Injector Fuel Concentration Map

6.2 Engine Tests

As mentioned in the Section 2.2, turbine testing at full load on 100% hydrogen using the hydrogen injectors with the standard natural gas liner initially resulted in NOx emissions of 181.4 ppmvd corrected to 15% O_2. In subsequent effort, Capstone supported UCI by swapping out the commercial natural gas liner with the commercial one used for liquid petroleum gas. The LPG liner featured partially blocked dilution jet holes which effectively increased the air flow to the fuel injectors. As shown in Figure 12, emissions decreased to 137.7 ppmvd corrected after changing the liner configuration to the LPG liner. The hydrogen results shown are an average of 3 runs, whereas the natural gas results are from 2 runs. Two of the hydrogen results with the LPG liner were taken one year apart. NOx values for each run are based on a 1 minute running average once the emissions readings reach steady state value.

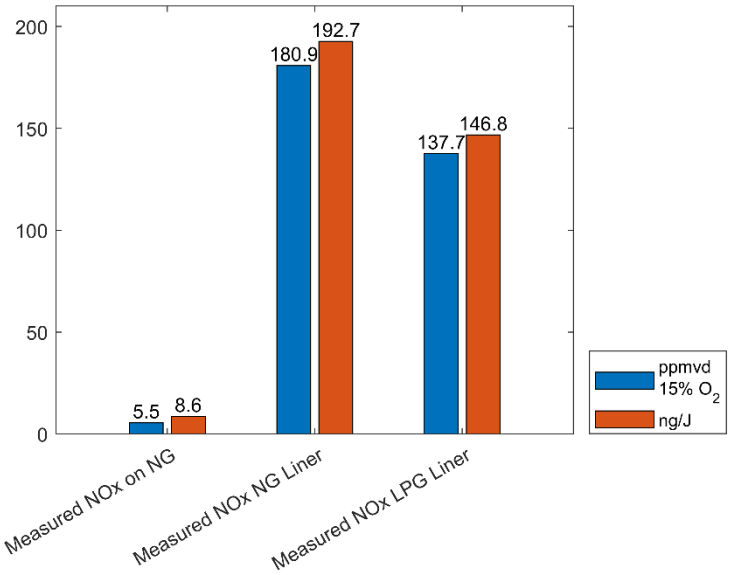

Figure 12. Full load average NOx emissions using hydrogen injectors compared with natural gas injectors used with natural gas liner.

The results shown in Figure 12 are from tests on different days, one of which is one year apart. This shows consistency in the emissions. The variability among the runs is about 1 ng/J for the hydrogen tests. As shown, levels for natural gas are significantly lower. But a key goal of these initial tests was to establish operability on pure hydrogen with less emphasis on emissions initially.

Under the current effort, additional testing was carried out in August 2023 to evaluate the emissions performance as a function of engine load. As shown, the NOx emissions does vary with load. This is associated with the fuel injector staging that occurs during load change. For example, up to about 20kW, two injectors are injecting fuel ("plane of two" in Figure 6). These injectors remain fueled and a third injector becomes fueled between 20 and 25kW. A fourth injector turns on between 35 and 40 kW and so forth. This results in a "sawtooth" pattern in the NOx emissions as shown in Figure 13. Due to the limited testing time afforded by use of hydrogen 6-paks (a 6 pak lasts approximately 30 minutes at full load) data were obtained at 5 kW increments. With finer increments the sawtooth pattern is clearer (e.g., [32]). The injector stage points can be user set in the software and represent a possible parameter to consider in systematic testing although that was beyond the current scope.

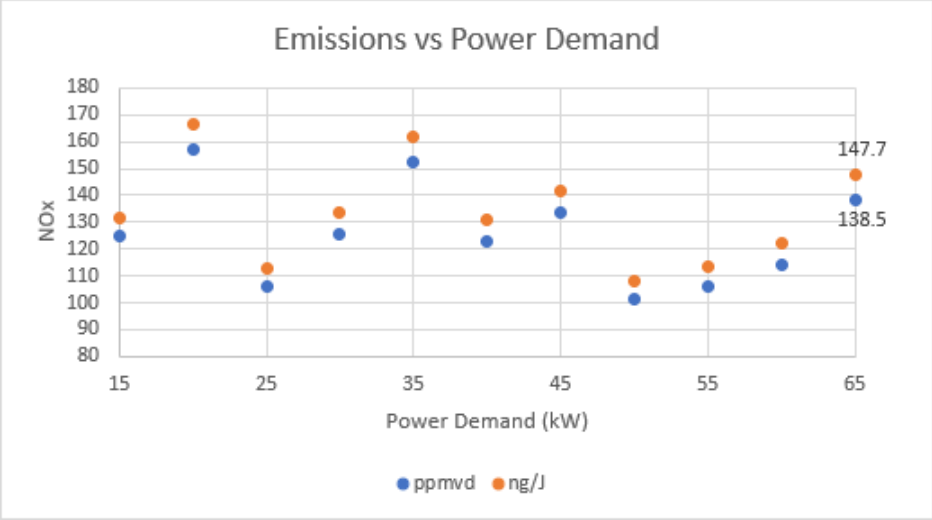

Figure 13. NOx Performance vs Load for Hydrogen Injectors with LPG liner and 100% Hydrogen.

6.3 NOx Inference from Mixing Studies.

To infer the NOx performance implied by the mixing levels, the reactor network shown in Figure 8 was used to compute the NOx emissions. For this work, GRIMech 3.0 was utilized for the 100% NG case and HyChem for the 100% H_2 case. GRIMech is widely used for natural gas chemical kinetic analysis. HyChem, while relatively recent, has been looked to for its ability to be used with mixtures of hydrogen and natural gas.

Initial predicted NOx values that do not include unmixedness, i.e., perfect mixing was assumed, are plotted and shown in Figure 14 to illustrate the effect of equivalence ratio on NOx emissions. Both y-axes are at the same range to show the bias of ppmvd in favor of natural gas. The difference between unit conversion is larger for natural gas than hydrogen.

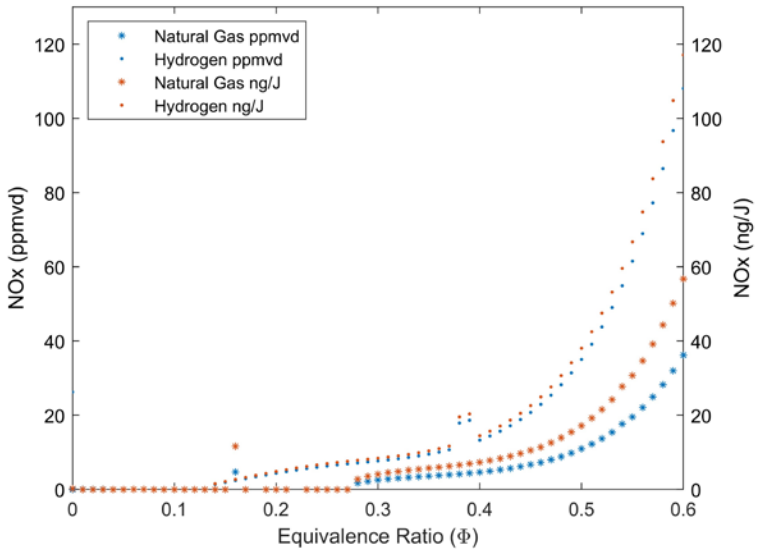

Figure 14. NOx Emissions vs. Equivalence Ratio

The amount of NOx produced by hydrogen combustion is higher than natural gas and begins to exponentially increase at a lower equivalence ratio. This is attributed to the higher flame temperature of hydrogen compared to natural gas at an equal equivalence ratio. However, the characteristics of hydrogen allow combustion at lower equivalence ratios compared to natural gas. This characteristic is exploited in the hydrogen injectors to make the fuel/air mixture leaner, thus lowering equivalence ratio, and to help reduce NOx emissions on pure hydrogen combustion.

The design of the hydrogen injectors has a shorter premix zone, reducing the residence time and the effectiveness of the mixing. The wide equivalence ratio distribution occurs at the injector exit plane due to this design. The fuel rich areas of the injector produce higher NOx emissions because of the higher equivalence ratios as shown in Figure 14.

The average level of measured concentration was normalized to the estimated overall injector equivalence ratio based on the fuel flow and understanding of air flow splits at full power. The variation in mixing from the measured values was then used to introduce unmixedness into the simulation. The area weighted equivalence ratio based on the measured values (from Figure 11) was used to establish a distribution of equivalence ratios for each injector as shown in Figure 15. Note the much wider range of local equivalence ratios observed for the high flame speed injectors. It is evidence from the relationship between NOx and equivalance ratio shown in Figure 14 that even small occurences of equivalence ratios above 0.5 will lead to significant increases in overall NOx. Hence the expectation is that, with the current injector performance for the high flame speed injector, the NOx levels will be higher than desired.

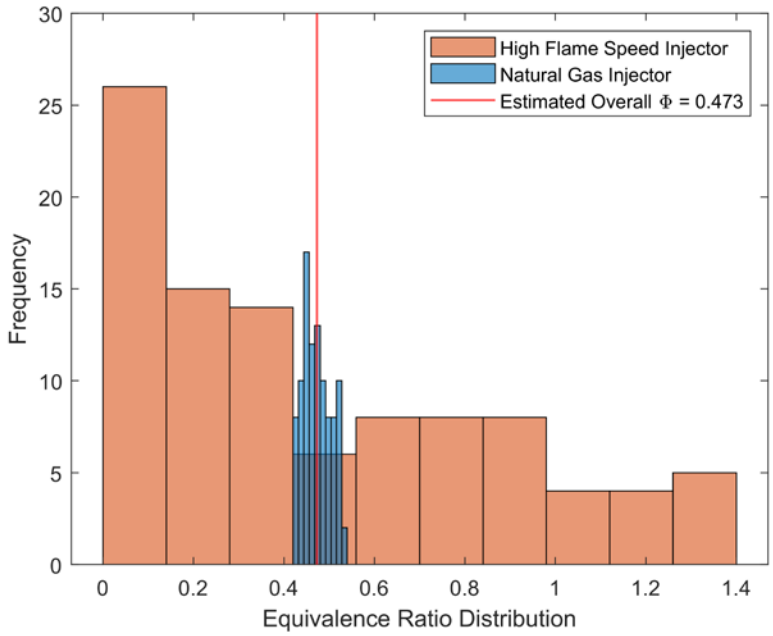

Figure 15. Injector Exit Plane Fuel Concentration Distribution.

The unmixedness of the injectors was quantified by performing a parameter study in the CRN with the corresponding equivalence ratios of each injector. Figure 16 shows the process for calculating NOx emissions with unmixedness using injector characterization and the CRN. Results for expected NOx were computed using this approach to add unmixedness to the fuel/air entering the combustor along with the reactor network.

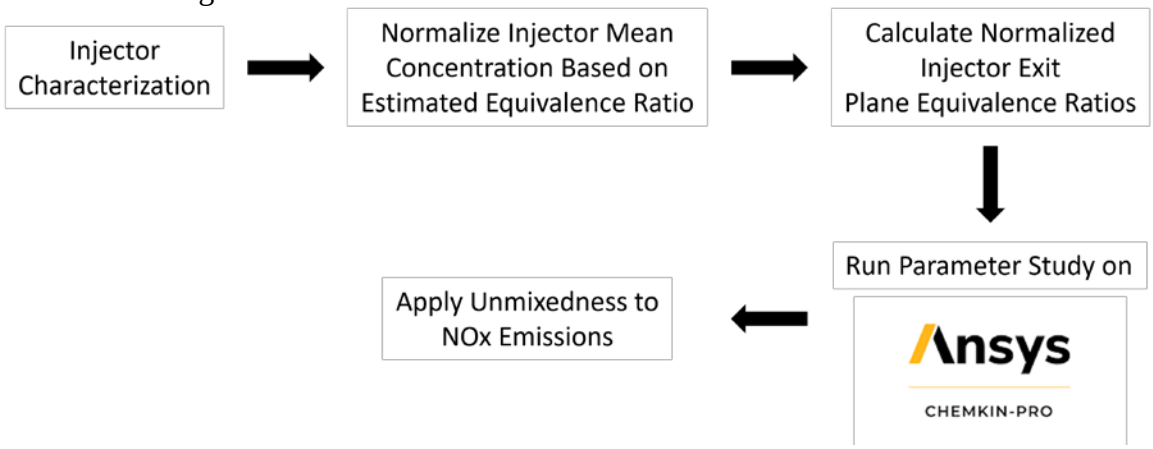

Figure 16. Flow Chart illustrating the NOx Inference process for the Engine.

6.3.1 Natural Gas Injectors/Natural Gas Liner

As shown in Table 4, predicted NOx emissions were 8.86 ppmvd @ 15% O2 for natural gas (using GRIMech 3.0), with the measured mixing for the natural gas injectors. If the mixing were perfectly uniform, the reactor network suggests NOx would be 8.27 ppmvd @ 15% O2. These values align well with measured values [32] and "Measured NOx" in Table 4 (5.77 ppm), but are subject to uncertainties with the actual fuel/air mixture in the injector as well as the chemical kinetic mechanism used. Regarding sensitivity to mechanism, NOx values for natural gas were

computed with 5 different reaction mechanisms operating at an estimated equivalence ratio of 0.473 corrected to 15% O_2 as shown in Table 4. The emissions are presented in both ppmvd and ng/J. As shown in Table 4, a nearly factor of 2 difference in predicted NOx is evident. This is attributed to differences in specific reaction parameters such as global activation energy and/or preexponential terms. Because there are hundreds of reactions (Table 3), small differences in values for several of the reactions lead to differences in NOx emissions. In this case, the UCSD mechanism matches most closely (7.56 ppm) with the measured NOx values of 5.77 ppm. Table 4 also presents results on a ng/J basis. This is done to provide a better comparison of NOx results between natural gas and hydrogen. As discussed in [29], the additional water produced by hydrogen when it burns compared to natural gas leads to higher concentration of exhaust species when presented on the typical dry basis..

Table 4. Predicted NOx Emissions based on Measured NG injector concentration data and "Perfect Mixing" Compared to Measured NOx Emissions

Reaction Mechanism:	Measured Mixing NOx corr. PPM/1	Perfect Mixing NOx corr. PPM	Measured Mixing NOx ng/J	Perfect Mixing NOx ng/J
Grimech 3.0	8.86	8.27	13.96	13.0
Aramcomech	13.23	12.46	20.78	19.58
UCSD	7.56	6.75	11.87	10.6
Konnov v0.5	17.44	16.35	27.39	25.69
HyChem 2.1	14.19	13.23	22.29	20.79
Measured NOx	5.77	NA	8.96	NA

/1 NOx corr indicates ppm on a dry basis corrected to 15% O2

The other take away from Table 4 is that, while the mixing performance of the natural gas injector is relatively good, the slight unmixedness present leads to a non-trivial increase in the NOx produced. As shown, NOx increases by about 1 ppm due to unmixedness (which translates into 5-10% differences. In consideration of Figure 5, however, it is evident that these NOx emissions are about as low as could be expected for lean premixed operation on natural gas. And directly tied to this mixing performance, this engine can attain the most severe NOx regulations including certification under California's DG certification program [5].

6.3.2 Hydrogen Injectors

As shown in Table 5, for hydrogen and the high flame speed injector (not accounting for the additional air admitted into the injector due to the increased overall area provided by the extra holes (recall Figure 4b)), the unmixedness associated with the hydrogen injector infers NOx levels of 343.87 ppmvd @ 15% O2 (e.g. with HyChem) at the estimated equivalence ratio of 0.473. If the injector attained fully premixed conditions, the NOx levels are estimated at 43.41 ppmvd @ 15% O2, or an 80% reduction. If the same equivalence ratio is used for hydrogen as for natural gas, the higher NOx levels for hydrogen are expected as the flame temperature for a fixed equivalence ratio is higher for hydrogen. If the additional water generated by hydrogen is accounted for (which drives the ppm values up on a dry basis), the 43.41 ppm would correspond to 31.7 ppm [29]. As discussed in [29], perhaps a better way to compare emissions for natural gas and hydrogen fuels is to use a mass emissions basis. As a result, Table 5 also presents emission in ng/J. To illustrate sensitivity to the mechanism used, Table 5 lists the emissions predicted by all the mechanisms used in this study (at least that yielded reasonable results). Mechanisms like GRIMech 3.0 can run using 100% hydrogen as the fuel, however, they yield results low single

digit NOx values (like the 100% methane cases) and are thus unreasonable. This is because Grimech 3.0 was designed for natural gas with modest levels of higher hydrocarbons.

Table 5. Predicted NOx Emissions based on Measured Hydrogen Injector concentration data and "Perfect Mixing" Compared to Measured NOx Emissions for Natural Gas Operating Condition

Reaction Mechanism at 0.473 ER:	Measured Mixing NOx corr. PPM/1	Perfect Mixing NOx corr. PPM/1	Measured Mixing NOx ng/J	Perfect Mixing NOx ng/J
HyChem 2.1	343.87	43.41	371.73	47.38
Galway-Syngas	390.68	75.92	422.42	82.85
Ansys H_2	345.35	55.30	373.35	60.34
Aramcomech	346.71	60.67	374.84	66.21
Measured (NG liner)	181.41	NA	193.16	NA

/1 NOx corr indicates ppm on a dry basis corrected to 15% O2

The predicted NOx emissions for perfect mixing are lower than the experimental values. However, the predicted emissions are higher than the experimental values if the measured mixing values are used and it is assumed that the same amount of air flows through both the natural gas and hydrogen injectors. Actually, the hydrogen injectors have more open area compared to the natural gas injectors, meaning that they operate under leaner conditions than the 0.473 equivalence ratio assumed in the analysis presented in Table 5. The additional air flowing into the hydrogen injectors can be estimated based on differences in open areas (recall Figure 4). It is noted that the actual injector average equivalence ratio is not independently known. It can be estimated from the physical open areas on the injector, liner, and dilution jets. However, there are modest leaks in the liner and the flow interaction and unknown flow discharge coefficients make the actual flow splits difficult to determine.

As a result, the reactor network was used in a different way to account for the extra air flowing for the hydrogen injectors. This involved adjusting the equivalence ratio until the predicted NOx emissions match the measured emissions levels. Table 6 shows predicted equivalence ratio (from each mechanism) required to match measured NOx levels achieved by the hydrogen injectors. The predicted decrease in average injector equivalence ratio due to the extra air admitted by the hydrogen injectors is 0.16 to 0.18 compared to the NG injectors. The values shown in Table 6 (0.311 based on HyChem) are within reason, but the actual values are not known.

Table 6. Equivalence Ratio prediction based on emissions using hydrogen injectors and NG Liner

Reaction Mechanism at (Φ) with NG liner:	Measured Mixing NOx corr. PPM/1	Perfect Mixing NOx corr. PPM	Measured Mixing NOx ng/J	Perfect Mixing NOx ng/J
HyChem 2.1 (0.311)	181.54	11.24	195.69	12.26
Galway-Syngas (0.294)	181.11	15.61	195.29	17.04
Ansys H_2 (0.310)	182.79	14.08	197.08	15.36
Aramcomech (0.308)	181.91	14.64	196.13	15.98
Measured (NG liner)	181.41	NA	193.16	NA

/1 NOx corr indicates ppm on a dry basis corrected to 15% O2

The next step was to evaluate how changing the combustor liner affected the NOx. The liner was changed from the NG to the LPG configuration in which the latter forces even more air through the injectors by blocking some of the downstream dilution holes which are used to cool the exhaust temperatures prior to entry into the turbine nozzle. This change further decreases the equivalence ratio in the combustion zone immediately downstream of the injectors. Table 7 shows the predicted equivalence ratio when the additional air due to changing the injectors *and* the combustor liner are considered in the CRN. As shown in Table 7, the measured NOx values do drop significantly (from 181 to 138 ppm).

Table 7. Equivalence Ratio prediction based on emissions using hydrogen injectors and LPG Liner

Reaction Mechanism at (Φ) with LPG liner:	Measured Mixing NOx corr. PPM/1	Perfect Mixing NOx corr. PPM	Measured Mixing NOx ng/J	Perfect Mixing NOx ng/J
HyChem 2.1 (0.290)	137.58	10.51	148.26	11.46
Galway-Syngas (0.275)	136.44	13.93	147.12	15.21
Ansys H_2 (0.288)	136.6	12.68	147.24	13.84
Aramcomech (0.287)	138.07	12.44	148.83	13.57
Measured (LPG liner)	137.71 (avg)	NA	146.81 (avg)	NA

/1 NOx corr indicates ppm on a dry basis corrected to 15% O2

The predicted equivalence ratio further decreases from 0.311 to 0.290 (based on HyChem) when the additional air through the injectors due to the LPG liner is considered. Also as shown, if perfect mixing could be achieved, the NOx emissions would decrease to nearly single digit values. On a ng/J basis, the NOx emissions are comparable to emissions achieved when operating on natural gas and thus illustrates the potential for attaining low NOx performance through improved mixing and redistribution of the air in the combustion liner/fuel injector.

In this case, an equivalence ratio of 0.29 does seem plausible for hydrogen. While far too lean to sustain combustion with natural gas, an equivalence ratio of 0.29 would result in a stable hydrogen reaction which illustrates a key feature of hydrogen to extend the operability range of the combustion system to very lean mixtures.

To this point, the reactor network used remained fixed in terms of size. Table 4 through Table 7 present results based on a "static" CRN, meaning that the same reactor volumes were used regardless of the fuel type for all cases. As discussed in [33], a static CRN can be used when the fuel composition of up to 30% hydrogen is mixed into NG. However, with more than 30-50% hydrogen addition, the reaction size changes noticeably based on both CFD and experiments. As a result, the residence time in the flame zone changes. To account for the smaller reaction zone for hydrogen, the volume of PSRs 2, 4, and 6 (recall Table 1) are decreased to $1/5^{th}$ that of the reactor used for natural gas. T$1/5^{th}$ was used because previous experiments have shown that the flame size of hydrogen is 3 to 7 times smaller than that of natural gas. The results shown in Table 8 are based on the smaller reactors. In this case, the predicted equivalence ratio increases to 0.366 (based on HyChem). Equivalence ratio predictions for each mechanism are tabulated in Table 8 for the variable size reactor network.

Table 8. Equivalence ratio prediction considering 1/5 flame size for hydrogen compared to NG with LPG liner

Reaction Mechanism at (Φ) with LPG liner:	Measured Mixing NOx corr. PPM/1	Perfect Mixing NOx corr. PPM	Measured Mixing NOx ng/J	Perfect Mixing NOx ng/J
HyChem 2.1 (0.366)	137.71	10.44	148.52	11.38
Galway-Syngas (0.332)	137.73	14.02	148.55	15.29
Ansys H_2 (0.364)	137.87	13.45	148.72	14.67
Aramcomech (0.361)	137.46	13.87	148.31	15.54
Measured (LPG liner)	137.71 (avg)	NA	146.81 (avg)	NA

/1 NOx corr indicates ppm on a dry basis corrected to 15% O2

As before, HyChem predicts the highest predicted equivalence ratio to match the measured NOx emissions at 0.366 and Galway-Syngas predicts the lowest at 0.332 for experimental turbine emissions. Again, these values seem plausible (perhaps more so than 0.29 value suggested by Table 7). Figure 18 summarizes the measured NOx values and the NOx inferred from the CRN simulations assuming the average injector equivalence ratio is 0.366.

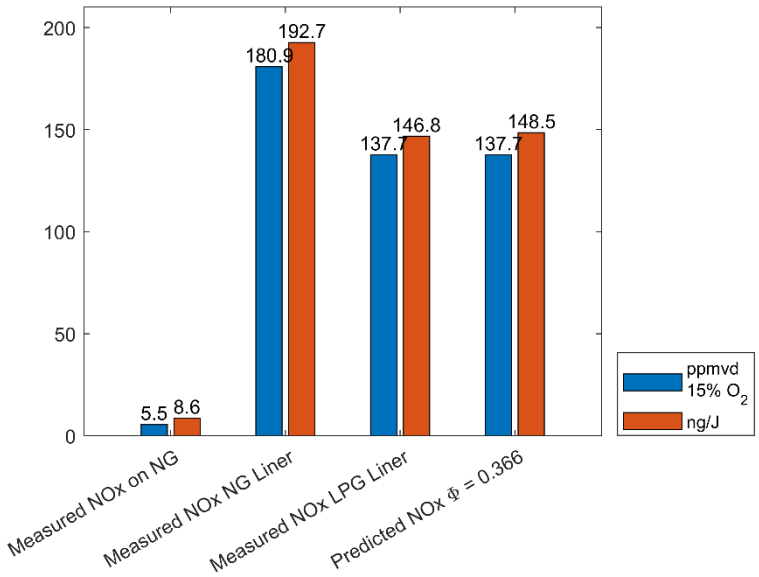

Figure 17. Comparison of Measured and Inferred NOx

NOx emissions for estimated equivalence ratios from 0 to 0.6 were calculated and plotted for the hydrogen and natural gas injectors to illustrate the effect of mixing on NOx emission. The results are shown in Figure 18. The effect that fuel rich areas at the injector exit plane have on emissions are emphasized by predicted NOx emissions with unmixedness versus NOx emissions with perfect mixing for both injector designs at various equivalence ratios. The natural gas injectors, which have well mixed fuel and air, resulted in small differences between actual (measured) and perfect NOx emissions. However, the results for the hydrogen injectors, which have poor mixing, resulted in large differences between perfect and actual (measured) mixing, illustrating how the large local equivalence ratios have a significant impact on NOx emissions.

a) Natural Gas Injector b) Hydrogen Injector

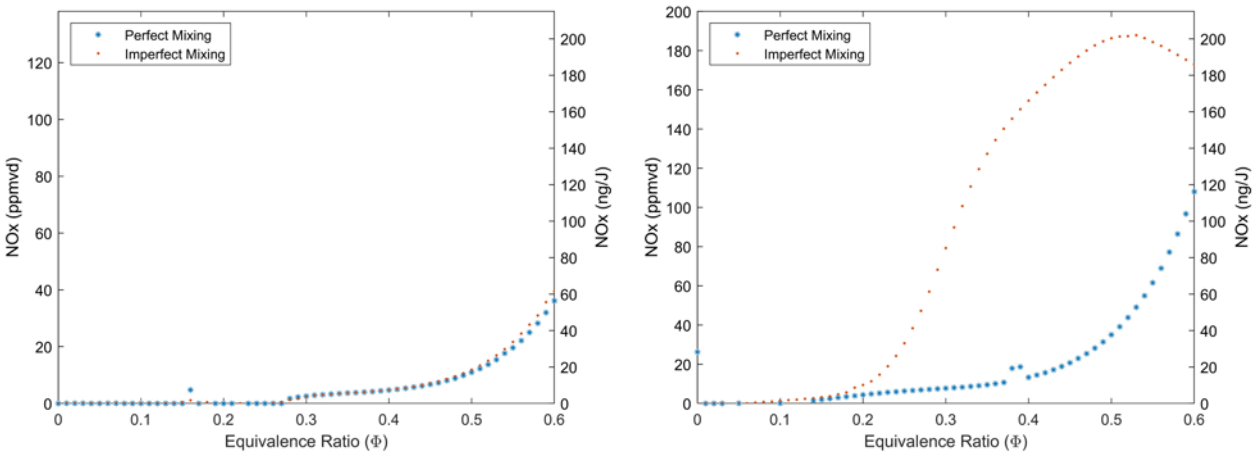

Figure 18. Predicted NOx Emissions vs Estimated Injector Equivalence Ratios

These plots were generated with data gathered from the CRN using GRIMech for methane and HyChem for hydrogen. For natural gas, the plot shows that the lowest equivalence ratio combustion happens is 0.28, however, carbon emissions increase with decreasing equivalence ratio. Hydrogen combustion does not produce carbon therefore the equivalence ratio can be decreased to 0.28 and even lower to about 0.1 as shown by Figure 18b.

6.4 Extended Injector Mixing Studies.

To explore the sensitivity of the mixing to injector modifications, a simple extension to one of the injectors was made. Essentially, the injector outer tube was extended by 1". This allows more distance/time for the fuel to mix with the air. This would represent a relatively straightforward modification to the injector. Figure 19 illustrates the temporary modification to extend the exit plane of the injector by 1 inch. This injector could not be run in the engine as it is just sealed with silicon. But the strategy works fine for doing the mixing studies and helps illustrate the value of the mixing rig coupled with the inferred NOx from the reactor network. This illustrates the practicality of using the mixing measurement to infer NOx emissions.

a) Baseline Hydrogen Injector b) Extended Hydrogen Injector

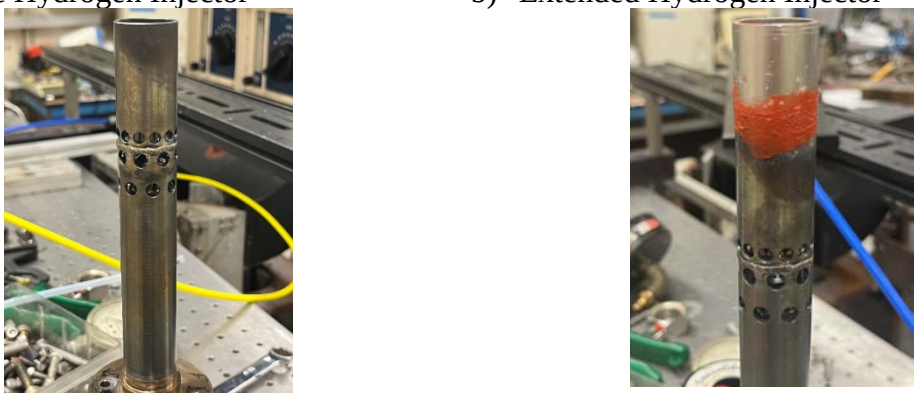

Figure 19. Baseline Injector and Extended Injector Configurations.

Figure 20 shows the measured velocity fields. The average velocity for the baseline hydrogen injector is 143.6 f/s with a standard deviation of 9.6 ft/s over the plane. With the extension added, the average velocity is 142.2 ft/s with a standard deviation of 11.0 ft/s. So the velocity field remains essentially unchanged.

Figure 21 shows the measured concentration fields. The average concentration for the baseline hydrogen injector is 5463 ppm with a standard deviation of 4646 ppm over the plane. With the extension added, the average concentration is 5117 ppm with a standard deviation of 3367 ppm over the plane. Hence the mixing is significantly improved.

a) Baseline Hydrogen Injector

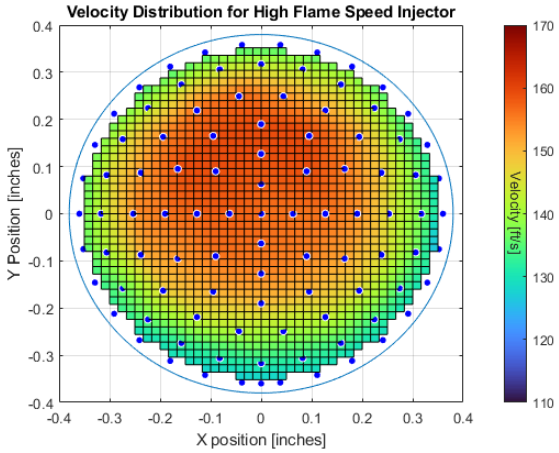

b) Extended Hydrogen Injector

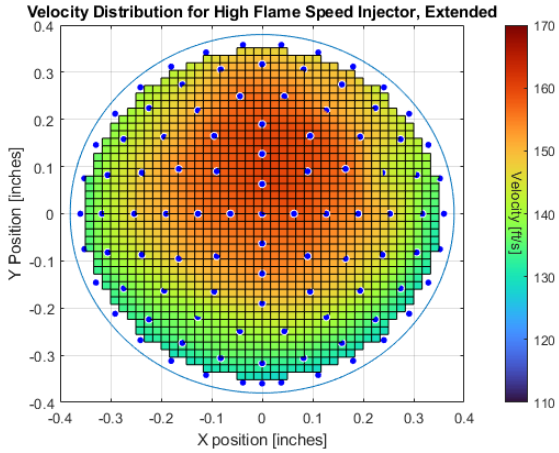

Figure 20. Velocity Field at Exit Plane.

a) Baseline Hydrogen Injector

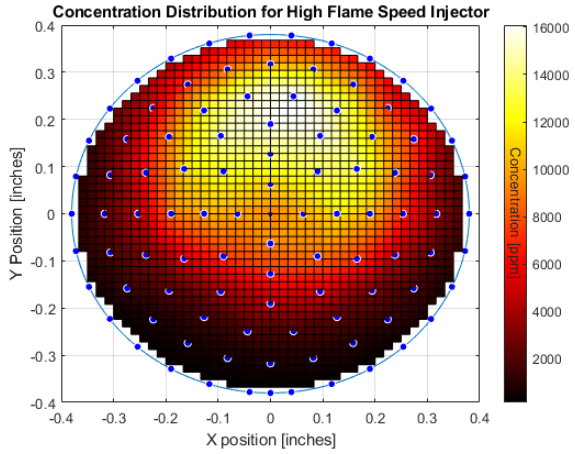

b) Extended Hydrogen Injector

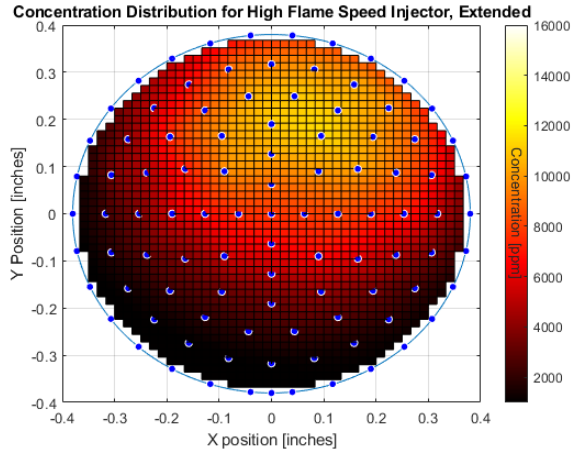

Figure 21. Concentration Measurements at Exit Plane.

To put the mixing performance in context with the CRN analysis and comparison with the baseline hydrogen injector and natural gas injector, Figure 22 presents the histogram of the equivalence ratios at the exit plane of the injectors for the baseline natural gas injector, the tested high flame speed injector, and the extended high flame speed injector. By extending the injector, the spread in equivalence ratio is reduced modestly.

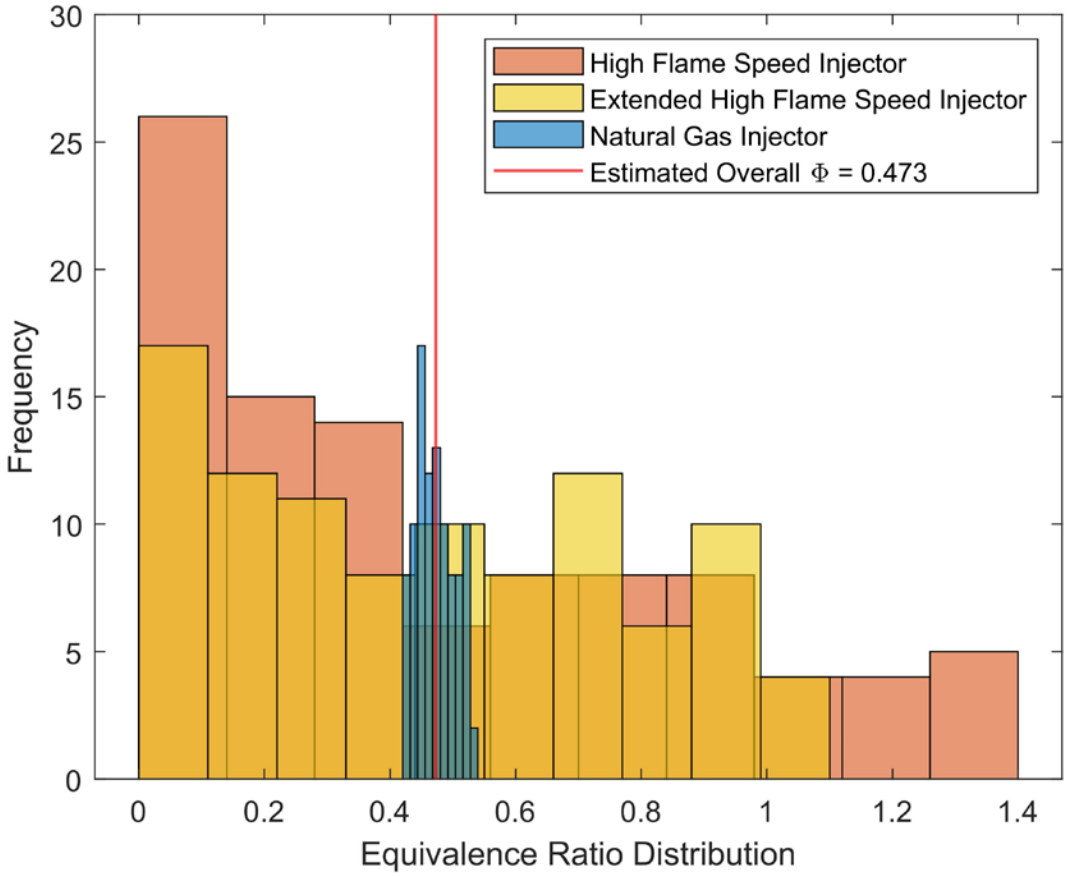

Figure 22. Distribution of Equivalence Ratios Measured at the Exit Plane of the Different Injector Configruations Studied.

Using the NOx inference approach above, the improved mixing is predicted to reduce the NOx from 138 ppm to 84.3 ppm. While this is higher that the fully mixed value, it does illustrate that a minor injector modification can potentially lead to a significant reduction in NOx. If perfect mixing could be attained, NOx levels of 10.4 ppm could potentially be attained.

Figure 23 summarizes the measured and inferred NOx results for the C65 engine operated on 100% hydrogen. As shown, the current effort has demonstrated a reduction in measured NOx by changing the liner from the standard natural gas liner to one developed for liquid petroleum gas. The use of the measured mixing profiles and the reactor network, modestly improving injector mixing would result in a significant reduction in NOx. By significantly improving the mixing additional NOx reductions can be attained resulting in levels that are comparable to those with natural gas. Further, with the inherent stability of hydrogen, it is believed that further leaning the injector out and/or altering fuel staging can also help with reducing NOx. The right most columns in Figure 23 show the case where the mixing attained with the hydrogen injectors can reach the mixing level of the natural gas injector and if the reaction zone equivalence ratio is reduced from 0.366 to 0.330 (which should be feasible with hydrogen), the same NOx levels (on a ng/J basis) attained with the commercial natural gas engine can be achieved. In addition, as demonstrated in

the previous project with SCG, changing the turbine exit temperature set point (recall Figure 3) is yet another adjustment that can be made to further reduce NOx.

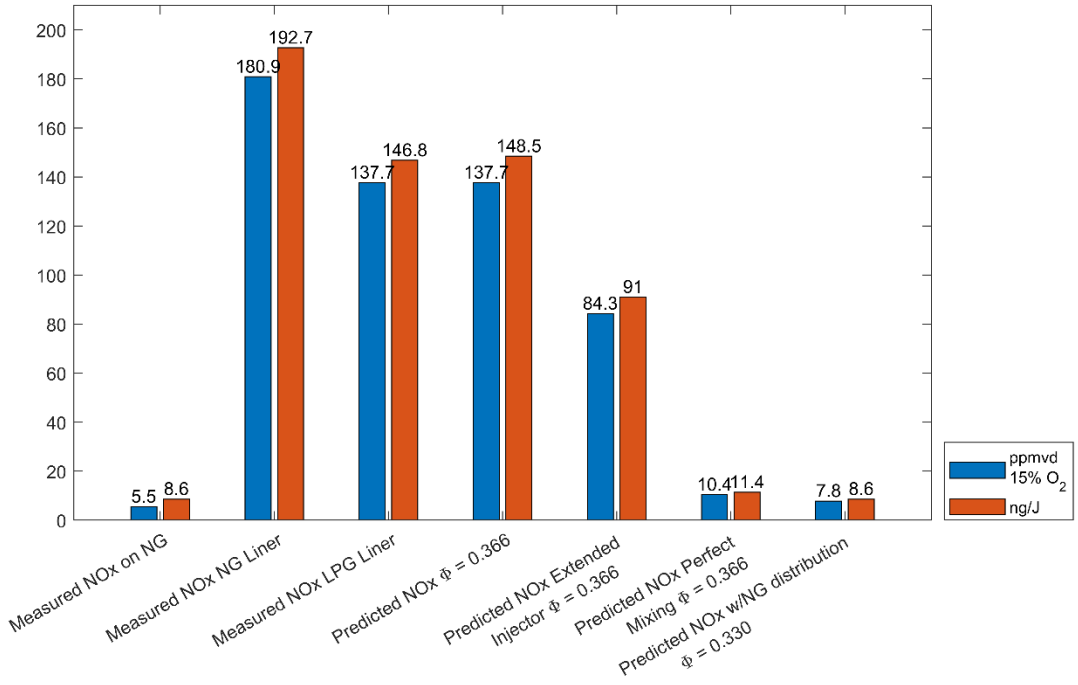

Figure 23. Summary of Full Load NOx Results (Measured and Predicted).

7 TECHNOECONOMIC ANALYSIS

There are 143 Capstone gas turbines in SoCal region with 15.3 MW output. Of those 143 engines, 75% are C65 units, which equates to 107 units. Potentially, should hydrogen be available, these engines could be retrofitted to operate on 100% hydrogen. A discussion on retrofit costs follows.

One cost estimate for hydrogen injectors was $2471.03 per injector using 3D printing methods. It is likely that injectors built using this method would not be able to withstand the conditions inside the engine, therefore, they would only be suitable for determining mixing capability. The injectors must be made by CNC machining for turbine operability. A set of 6 CNC machined injectors has been quoted at $~14,000 by Capstone's supplier. This represents a "one-off" price and presumably, if injectors were made in larger quantities the per unit cost would drop significantly. This high-volume cost is estimated to be similar to that of the commercial natural gas injectors. The liner used is commercially available, though further modifications may be required to further reduce NOx emissions. Regardless, the cost of the liner compared to the natural gas liner is expected to be similar.

As a result, it would cost about $1,819,000 (107 C65 units x $17,000 for set of 6 injectors) to make hydrogen injectors for all the C65 units in the SoCal region at the quoted price.

In terms of emissions performance, the C-60 Capstone engine, which is the same as the C65, has reported criteria pollutant and greenhouse gas emissions as low as 3.13 and 3.53 ppmvd at 15% O_2 for NOx and CO, respectively, operating at full load and with maximized heat recovery

[44]. According to [44], on a yearly basis, the amount emissions of all the operational C65 engines in the SoCal region equates to 14,977, 10,354, and 154,802,340 lbs/yr for NOx, CO, and CO_2, respectively. It is not clear exactly how the 14,977 lbs/yr value was attained in [44]. In the current effort, the measured NOx levels for natural gas were 5.7 ppmvd @ 15% O2 or 8.96 ng/J. Using these measured values, UCI estimates the NOx emissions for natural gas are 7,148 lbs/yr. In the current effort, the lowest amount of emission achieved, operating on 100% H_2, was 137 ppmvd for NOx. This equates to 117,124 lbs/yr. Compared to NG, the amount of NOx increases by 102,147 lbs/yr. However, CO and CO_2 emissions are essentially eliminated. A 100% reduction of 154,812,694 lbs/yr in CO and CO_2 emissions.

As discussed herein, considerable reduction in NOx emission can be attained through improved fuel/air mixing, combustor liner modifications, and user-controlled settings in the software (e.g., turbine exit temperature set point). Especially for hydrogen, more air can be added to the lean out the combustion regions because of its high flammability. In the present work, the minimum reaction zone equivalence ratio reaction zone considered is 0. 366. But with hydrogen this could be reduced further, thereby driving NOx emissions down even further. Within the constraints of the current study (hydrogen injector, LPG liner, improved mixing), the NOx emissions with hydrogen can potentially be reduced to 9,080 lb/yr, which is still slightly higher than for natural gas. Again, this is based on a reaction zone equivalence ratio 0.366. If further modifications to the liner and/or injector to further lean out the reaction zone, it is expected that the NOx emissions could be reduced to levels below what is attainable on Natural gas.

To summarize the potential for the current study with constrains of LPG liner, hydrogen injectors, and baseline TET setpoints, Table 9 summarizes the yearly emissions for several cases considered at an equivalence ratio of 0.366 for the predicted hydrogen cases. As shown, there is potential for the NOx emissions from a hydrogen fueled microturbine to be less than the present natural gas fired units which would reflect an improvement in air quality. That combined with the elimination of CO and CO2 represent a significant public benefit. To put the NOx numbers into context, SCAQMD estimates all sources in the basin will emit 184 tons per day [45] . The NOx emissions from the hydrogen fueled engines would generate 0.012 tons per day. Again, it is expected that NOx emissions below those emitted by natural gas fueled units can be attained through the features of hydrogen and further adjustments to the combustion liner and fuel injectors.

Table 9. Relative GHG and Pollutant Emissions for Hydrogen Fueled Engine vs Natural Gas Fired Engine.

Species (lbs/yr)	NG Fuel, NG Injectors and Liner	H_2 Fuel and H_2 Injectors, NG Liner	H_2 Fuel and H_2 Injectors, LPG Liner	Predicted, H_2 Fuel, Extended H_2 Injectors, LPG Liner (Φ=0.366)	Predicted, H_2 Fuel, Perfect Mixing, LPG Liner (Φ=0.366)
NOx	7,148	154,103	117,124	72,630	9,080/1
CO	10,354	0	0	0	0
CO_2	154,802,340	0	0	0	0

/1 as shown in Figure 23, it is believed that NOx levels equivalent to natural gas can be attained in which case the NOx increase associated with implementation of the 100% hydrogen C65 could be zero..

In terms of cost of electricity costs, the DOE is currently focused on developing technologies that can produce hydrogen with net-zero-carbon pathways at $1/kg by 2031, which on an energy

basis is $7.40/MMBtu. Cost of natural gas ranges from $2.59 to $4.31 per MMBtu according to Lazard's levelized cost of energy from April 2023 [46]. The US energy information administration [47], eia.gov, provides the cost of natural gas per MMBtu for the southern California region plotted throughout the year. In 2023 the price reached lows of $1.50/MMBtu and highs of $24.51/MMBtu during winter months. However, the price was usually between $2 to $4 per MMBtu for most of 2023. As a result, the cost of fuel, if unburdened by a carbon tax or such, may be slightly higher for hydrogen which would translate into higher energy costs.

8 SUMMARY AND RECOMMENDATIONS

8.1 Summary

The project successfully updated the facility infrastructure for safe use of 100% hydrogen in the C65 engine. The infrastructure can also potentially be used for the C-200 engine. Engine tests were carried out over a range of loads with 100% hydrogen and the measured values repeated to within 1% of the previous results obtained a year before. A test rig for quantifying injector mixing performance was established and used to quantify the mixing performance of both the natural gas injectors and the hydrogen injectors. The velocity results affirmed the design for high hydrogen allows more air flow into the injector as evidenced by the higher velocities overall. The results also indicated that the mixing performance of the hydrogen is much worse than the natural gas injector. The natural gas injector mixing performance is nearly perfect, which corresponds to the measured NOx levels corresponding to the expected entitlement levels based on Leonard and Stegmaier. The higher NOx levels for the hydrogen injector are a result of the relatively poor mixing. A small modification to the injector was shown to significantly improve mixing and a design for this approach should be fabricated and tested in the engine. A simulation strategy was developed to infer how the mixing performance affects NOx emissions. This tools provides a time efficient manner by which to test single injector concepts for mixing and velocity and thus guide design work towards a low emissions concept. This can be complimented by CFD to assist in optimization of the design to reach NOx emissions comparable to those for natural gas.

8.2 Recommendations

Based on the current results, there are several recommendations:

- As illustrated by the NOx inference results, improved mixing in the injector should result in reduced NOx. A conceptual design for the improved injector has been developed with Capstone and it would be a good next step to fabricate a set of improved injectors and make emissions measurements in the engine to affirm the improvement in NOx that is inferred from the simulation work.
- Modifications to the liner to force even more air into the injector should be explored as a means to further reduce NOx. The inherent stability of hydrogen should facilitate stable operation with significantly more air that is currently being injected.
- Establish CFD to simulate the injector design mixing and velocity fields. This would be spot checked with measured values on limited builds of the injector to identify promising designs for low emissions.
- A systematic TET parameter study should be carried out to understand how much NOx reduction can be provided by reducing the TET while at the same time ensuring minimum derate of the engine.

- A question regarding unburned hydrogen ("hydrogen slip") is worth examining. This requires the use of specialized equipment specifically targeting hydrogen in the exhaust gas. At some point, a trade off in NOx and unburned hydrogen is likely to be observed.

9 REFERENCES

1. Flores, R.J., Shaffer, B.P, and Brouwer, J. (2014). Dynamic Distributed Generation Dispatch Strategy for Lowering the cost of Building Energy, Applied Energy, Vol 123, pp 196-208.
2. Rist, J.F., Dias, M.F., Palman, M., Zelazo, D., and Cukurel, B. (2017). Economic Dispatch of a Single Micro-Gas Turbine under CHP Operation, Applied Energy, pp 1-18.
3. Kim, M.J., Kim, T.S., Flores, R.J., and Brouwer, J (2020). Neural-Network Based Optimization for Economic Dispatch of Combined Heat and Power Systems, Applied Energy, Vol 265, pp 114785
4. Flores, R.J. and Brouwer, J. (2018). Optimal Design of a Distributed Energy Resource System that Economically Reduces Carbon Emissions, Applied Energy, Vol 232, pp 119-138.
5. Distributed Generation Certification Program (2023), accessed November 14, 2023, https://ww2.arb.ca.gov/our-work/programs/dgcert/exec-orders
6. Lieuwen, T., McDonell, V., Petersen, E., and Santavicca, D. (2008). Fuel Flexibility Influences on Premixed Combustor Blowout, Flashback, Autoignition, and Stability, J. Engr Gas Turbines and Power, Vol 130(1): 011506.
7. Beerer, D. and McDonell, V. (2008). Autoignition of Hydrogen and Air in a Continuous Flow Reactor with Application to Lean Premixed Combustion, J. Engr Gas Turbines and Power, Vol 130(5): 051507.
8. Kalantari, A. and McDonell, V. (2017). Boundary Layer Flashback of Non-Swirling Premixed Reactions: Mechanisms, Fundamental Research and Recent Advances, Prog in Energy and Combustion Science, Vol 189 (12), pp 2115-2134.
9. Cadorin, M., Pinelli, M., Vaccari, A., Calabria, R., Chiarello, F., Massoli, P. and Bianchi, E. (2012). Analysis of a Micro Gas Turbine fed by Natural Gas and Synthesis Gas: MGT Test Bench and Combustor CFD Analysis, Vol 134, pp 071401.
10. Cappalletti, A., Martelli, F, Bianchi, E., and Trifoni, E. (2014). Numerical Retrofit of 100kW MGT combustor for 100% H2 fueling. Energy Procedia, Vol 45, pp 1412-1421.
11. Di Nardo, A., Bo, A., Calchetti, G., Giacomazzi, E., and Messina, G. (2020). Study on the Fuel Flexibility of a Microgas Turbine Combustor Burning Different Mixtures of H2, CH4, and CO2, J. Engr Gas Turbines and Power, Vol 142(6): 061001.
12. Pappa, A., Bricteux, L., Benard, P. and De Paepe (2021). Can Water Dilution Avoid Flashback on a Hydrogen-Enriched Micro-Gas Turbine Combustion?: A Large Eddy Simulations Study, J. Engr Gas Turbines and Power, Vol 143(4): 041008
13. Bauer, S., Hampel, B., and Sattelmayer, T. (2017). Operability Limits of Tubular Injectors with Vortex Generators for a Hydrogen-Fueled Recuperated 100kW Class Gas Turbine. J. Engr Gas Turbines and Power, Vol 139(8), pp 082607.
14. Zornek, T., Mosbach, T., and Aigner, M. (2019). Optical Measurements of a Lower Calorific Values-Combustor Operated in a Micro Gas Turbine with Various Fuel Compositions, . J. Engr Gas Turbines and Power Vol 141(4), pp 041032.
15. Wünning, J.A., and Wünning, J.G. (1992). Burners for Flameless Oxidation with Low NOx Formation even at Maximum Air Preheat, Gaswärme International, Vol 41(10< pp 438-444.

16. Lammel, O., Schütz, H., Schmitz, G., Lückerath, R., Stöhr, M., Noll, B., Ainger, M., Hase, M., and Krebs, W. (2010). FLOX Combustion at High Power Density and High Flame Temperatures, J. Engr Gas Turbines and Power, Vol 132, pp 1215031:9.
17. Therkelsen, P, Wertz, T.J., McDonell, V.G., and Samuelsen, G.S. (2009). Analysis of NOx Formation in a Hydrogen fueled Gas Turbine Engine. J. Engr Gas Turbines and Power, Vol 131(3), pp 031507.
18. Brucker-Kalb, J., Krosser, M., Hirsch, C., and Sattelmayer, T. (2010). Emissions Characteristics of a Premixed Cyclic-Periodical-Mixing Combustor Operated with Hydrogen-Natural Gas Fuel Mixtures, J. Engr Gas Turbines and Power, Vol 132(2), pp 021505.
19. Page, D., Shaffer, B., and McDonell (2012). Establishing Operating Limits in a Commercial Lean Premixed Combustor Operating on Synthesis Gas Pertaining to Flashback and Blowoff. Paper GT2012-69355, TurboExpo 2012, Copenhagen, Denmark.
20. (2002). C65 Microturbine [online]. Capstone Tubine Corp., 2020, C65+ICHP+Natural+Gas+CARB.pdf (d1io3yog0oux5.cloudfront.net)
21. Kalantari, A., Sullivan-Lewis, E., McDonell, V. (2016). Application of a Turbulent Jet flame Flashback Propensity Model to a Commercial Gas Turbine Combustor, J. Engr Gas Turbines and Power, Vol 139(4), p 04506.
22. C65+HPNG_331035E_lowres.pdf (d1io3yog0oux5.cloudfront.net), accessed Jan 4, 2024
23. Hydrogen Microturbine :: Capstone Green Energy Corporation (CGRNQ), accessed Jan 4, 2024
24. Chen, J, Mitchell, M., Nourse, J., and McKeirnan, R (2016). Flashback-Reducing Fuel Injector, International Patent WO 2016/018483 A1.
25. V.J. A. Kalantari, V. McDonell, S. Samuelsen, S. Farhangi, and D. Ayers, Towards improved boundary layer flashback resistance of a 65kw gas turbine with retrofittable injector concept (2018). Paper GT2018-75834, Proceedings of ASME TurboExpo 2018, Oslo, Norway, 2018, June
26. Lyons, Fuel/Air Nonuniformity—Effect on Nitric Oxide Emissions, AIAA J. 20(5):660–665 (1982)
27. T.F. Fric, Effect of Fuel-Air Unmixedness on NOx Emissions, AIAA 92-3345, 1992.
28. G. Leonard and J. Stegmaier, "Development of an aeroderivative gas turbine dry low emission combustion system," Journal of Engineering Gas Turbine Power , vol. 116, pp. 542-546, 1994
29. C.M. Douglas, S.L. Shaw, T.D. Martz, R.C. Steele, D. Noble, B.L. Emerson, and T.C. Lieuwen, Pollutant emisssions reporting and performance considerations fr hydrogen-hydrocarbon fuels in gas turbines, J. Engr. for Gas Turbines and Power, Vol 144 (9), pg 091003, 2022
30. V.G. McDonell, Lean Combustion in Gas Turbines, 2nd Edition (2016). In Lean Combustion—Technology and Control, edited by D. Dunn-Rankin, Academic Press, San Diego.
31. R. Tacina. Low NOx potential of gas turbine engines, Paper AIAA-90-0550, 28th Aerospace Sciences Meeting, 1990, Reno NV
32. V.M.Phi, J.L. Mauzey, V.G. McDonell, and G.S. Samuelsen, fuel injection and emissions characteristics of a commercial microturbine generator. Presented at 2004 Turbo EXPO, Paper GT-2004-54039, Vienna, Austria, 2004, June
33. A.F. Colorado and V.G. McDonell, reactor network analysis to assess fuel composition effects on NOx emissions from a recuperated gas turbine (2014). Paper GT2014-26361, TurboExpo 2014, Dusseldorf, Germany, 2014, 16-20 June

34. ANSYS Chemkin-Pro (2021).
35. Smith, G.P., Golden, D.M., Frenklach, M., Moriarty, N.W., Eiteneer, B., Goldenberg, M., Bowman, C.T., Hanson, R.K., Song, S., William C. Gardiner, J., Lissianski, V. V., Qin, Z., n.d. GRI-MECH 3.0
36. Y. Zhang, O. Mathieu, E.L. Petersen, G. Bourque, H.J. Curran (2017). Assessing the Predictions of a NOx Kinetic Mechanism using Recent Hydrogen and Syngas Experimental Data" Combustion and Flame 182, 122–141.
37. F. H. V. Coppens, J. De Ruyck, and A. A. Konnov, "The effects of composition on burning velocity and nitric oxide formation in laminar premixed flames of CH4 + H2 + O2 + N2," Combustion and Flame, vol. 149, no. 4, pp. 409–417, Jun. 2007
38. "Chemical Mechanism: Combustion Research Group at UC San Diego." https://web.eng.ucsd.edu/mae/groups/combustion/mechanism.html
39. C-W. Zhou, Y. Li, U. Burke, C. Banyon, K.P. Somers, S. Khan, J.W. Hargis, T. Sikes, E.L. Petersen, M. AlAbbad, A. Farooq, Y. Pan, Y. Zhang, Z. Huang, J. Lopez, Z. Loparo, S.S. Vasu, H.J. Curran "An experimental and chemical kinetic modeling study of 1,3-butadiene combustion: Ignition delay time and laminar flame speed measurements" Combustion and Flame 197 (2018) 423–438.
40. K. Wang, R. Xu, T. Parise, J. Shao, A. Movaghar, D.J. Lee, J. Park, Y. Gao, T. Lu, F.N. Egolfopoulos, D.F. Davidson, R.K. Hanson, C.T. Bowman, H. Wang, A physics-based approach to modeling real-fuel combustion chemistry - IV. HyChem Modeling of Combustion Kinetics of a Bio-derived Jet Fuel and Its Blends with a Conventional Jet A, Combustion and Flame 198 (2018) 477–489.
41. Breer, B., Rajagopalan, H, Godbold, C., Johnson II, H., Emerson, B., Acharya, V., Sun, W., Noble, D., and Lieuwen, T. (2023), Numerical Investigation of NOx Production from Premixed Hydrogen/Methane Fuel Blends, Combustion and Flame, Vol 255, pp 112920.
42. Glarborg, P., Miller, J., Ruscic, B, and Klippenstein, S., (2018). Modeling Nitrogen Chemistry in Combustion, Progress in Energy and Combustion Science, Vol 67, pp 31-68.
43. *PG-350E Portable Gas Analyzer - HORIBA*. (n.d.). Www.horiba.com. Retrieved June 10, 2021, from https://www.horiba.com/it/process-environmental/products/combustion/transportable/details/pg-350e-portable-gas-analyzer-19617
44. Piccot and McKinnon (2003). ETV Joint Verification Statement, Natural Gas Fired Microturbine Combined with Heat Recovery System—Capstone C60 Microturbine System. GHG Center and US EPA.
45. AQMD: Draft 2022 Air Quality Management Plan.
46. https://www.lazard.com/media/typdgxmm/lazards-lcoeplus-april-2023.pdf
47. https://www.eia.gov/special/disruptions/socal/winter/